19930092822 L-7

ARR L4J05

NATIONAL ADVISORY COMMITTEE FOR AERONAUTICS

WARTIME REPORT

ORIGINALLY ISSUED

October 1944 as

Advance Restricted Report L4J05

WIND-TUNNEL INVESTIGATION OF AN NACA 23021 AIRFOIL WITH A 0.32-AIRFOIL-CHORD DOUBLE SLOTTED FLAP

By Jack Fischel and John M. Riebe

Langley Memorial Aeronautical Laboratory
Langley Field, Va.

NACA

WASHINGTON

NATIONAL ADVISORY COMMITTEE FOR AERONAUTICS

ADVANCE RESTRICTED REPORT

WIND-TUNNEL INVESTIGATION OF AN NACA 23021 AIRFOIL WITH A 0.32-AIRFOIL-CHORD DOUBLE SLOTTED FLAP

By Jack Fischel and John M. Riebe

SUMMARY

An investigation was made in the LMAL 7- by 10-foot wind tunnel of an NACA 23021 airfoil with a double slotted flap having a chord 32 percent of the airfoil chord (0.32c) to determine the aerodynamic section characteristics with the flaps deflected at various positions. The effects of moving the fore flap and rear flap as a unit and of deflecting or removing the lower lip of the slot were also determined.

Three positions were selected for the fore flap and at each position the maximum lift of the airfoil was obtained with the rear flap at the maximum deflection used at that fore-flap position. The section lift of the airfoil increased as the fore flap was extended and maximum lift was obtained with the fore flap deflected 30° in the most extended position. This arrangement provided a maximum section lift coefficient of 3.31, which was higher than the value obtained with either a 0.2566c or a 0.40c single-slotted-flap arrangement and 0.25 less than the value obtained with a 0.40c double-slotted-flap arrangement on the same airfoil. The values of the profile-drag coefficient obtained with the 0.32c double slotted flap were larger than those for the 0.2566c or 0.40c single slotted flaps for section lift coefficients between 1.0 and approximately 2.7. At all values of the section lift coefficient above 1.0, the 0.40c double slotted flap had a lower profile drag than the 0.32c double slotted flap. At various values of the maximum section lift coefficient produced by various flap deflections, the 0.32c double slotted flap gave negative section pitching-moment coefficients that were higher than those of other slotted flaps on the same airfoil. The 0.32c double slotted flap gave approximately the same maximum section lift coefficient as, but higher profile-

drag coefficients over the entire lift range than, a similar arrangement of a 0.30c double slotted flap on an NACA 23012 airfoil.

INTRODUCTION

The National Advisory Committee for Aeronautics has undertaken an extensive investigation of various high-lift devices in order to furnish information applicable to the aerodynamic design of wing-flap combinations that will improve the safety and performance of airplanes. For use in take-off and initial climb, a high-lift device capable of producing high lift with low drag is desirable. For use in landings, however, high lift with variable drag is believed desirable. Other desirable characteristics are: no increase in drag with the flap neutral, small change in pitching moment with flap deflection, low forces required to operate the flap, and freedom from possible hazard due to icing.

The results of various investigations on the NACA 23021 airfoil are presented in references 1, 2, and 3. Results for the NACA 23021 airfoil with a single slotted flap having a chord 25.66 percent of the airfoil chord (0.2566c) are given in reference 1; results for the same airfoil with a 0.40c single slotted flap and with a 0.40c double slotted flap are given in references 2 and 3, respectively.

The present investigation, in which tests were made of a 0.32c double slotted flap on the NACA 23021 airfoil (fig. 1), is a continuation of the investigation reported in reference 4 of a 0.30c double slotted flap on an NACA 23012 airfoil.

APPARATUS AND TESTS

Models

An NACA 23021 airfoil with a 3-foot chord and a 7-foot span was the basic model used in these tests. The ordinates for the NACA 23021 airfoil section are given in table I. The airfoil was constructed of laminated mahogany and tempered wall board and is the same airfoil previously used for the investigations reported in references 1, 2, and 3. The trailing-edge section of the model ahead of the flaps was equipped with lips of steel plate rolled to the airfoil contour and extending back to the rear flap in order to provide the basic airfoil contour when the flaps were retracted (fig. 1).

The double slotted flap consisted of a fore flap and a rear flap. The fore flap (0.1467c) tested was the same one designated fore flap B in the investigation reported in reference 4 and had an upper surface and trailing-edge of dural and a lower surface of laminated wood. The fore-flap profile is shown in figure 1 and its ordinates are given in table I. The rear flap (0.2566c) tested was the one used in the investigations reported in references 1 and 3. Its profile is also shown in figure 1 and the ordinates are given in table I.

Both the fore flap and the rear flap were attached to the main part of the airfoil by special fittings that permitted them to be moved and deflected independently. Each flap also pivoted about its own nose point at any position; increments of 5° deflection were provided for the fore flap and increments of 10° deflection for the rear flap. The nose point of either flap is defined as the point of tangency of the leading-edge arc and a line drawn perpendicular to the flap chord. The deflection of either flap was measured between its respective chord and the chord of the main airfoil. The model was made to a tolerance of ±0.015 inch.

Tests

The model was mounted vertically in the closed test section of the LMAL 7- by 10-foot tunnel and completely spanned the jet except for small clearances at each end. (See references 5 and 6.) The main airfoil was rigidly attached to the balance frame by torque tubes that extended through the upper and lower boundaries of the tunnel. The angle of attack of the model was set from outside the tunnel by rotating the torque tubes with a calibrated electric drive. This type of installation closely approximates two-dimensional flow and the section characteristics of the model being tested can therefore be determined.

A dynamic pressure of 16.37 pounds per square foot was maintained for most of the tests but, as the flaps were extended and the rear-flap deflection was increased to 60° and 70°, it was necessary to reduce the dynamic pressure because of the limited power of the tunnel motor. With the configuration for maximum lift, a dynamic pressure of 14.84 pounds per square foot was maintained. These dynamic pressures correspond to velocities of 80 and 76.2 miles per hour under standard sea-level conditions and to average test Reynolds numbers of approximately 2.245×10^6 and 2.140×10^6, respectively. Because of the turbulence in the wind tunnel, the effective Reynolds numbers R_e (reference 7) were approximately 3.6×10^6 and 3.42×10^6, respectively. In each case, R_e is based on the chord of the airfoil with the flaps retracted and on a turbulence factor of 1.6 for the LMAL 7- by 10-foot wind tunnel.

No tests were made of the plain airfoil nor of the model with the flaps completely retracted because the characteristics of the plain airfoil had previously been investigated and reported in reference 1.

The optimum flap positions for the various flap deflections were considered, for purposes of making the best selection, to be the positions at which either maximum lift, minimum drag, or minimum pitching moment was obtained, although, as previously indicated, a variable drag is desired for landing conditions.

Three positions of the fore flap were selected in determining various extended positions of the flaps or a possible path for the extension of the flaps. The least extended fore-flap position, having a 5° deflection (position 1), and the chordwise location of the intermediate position (position 2) were chosen arbitrarily. The location perpendicular to the chord and the 20° deflection for position 2 were optimum as determined from a maximum-lift survey with the rear flap deflected 50° and 60°. Because of the large number of tests involved in determining the optimum-lift position of the double slotted flap, a preliminary survey was made to determine the optimum position and deflection of the most extended position (position 3) of the fore flap with the rear flap deflected 60° and 70° at various positions. Tests were thereafter made with the fore flap at each of the three selected positions in order to determine the maximum lift and the optimum position of the rear flap at several deflections. Data were obtained for rear-flap deflections of 10°, 20°, 30°, and 40° at position 1; 30°, 40°, 50°, and 60° at position 2; and 40°, 50°, 60°, and 70° at position 3. Inasmuch as it appeared likely that only small rear-flap deflections would be used with the least extended fore-flap position and that only large rear-flap deflections would be used with the most extended fore-flap position, the tests were confined to these configurations. In order to determine the effect on the aerodynamic characteristics, tests were also made with the lower lip of the slot in its normal position on the contour, deflected 19° within the airfoil contour (at fore-flap position 2), and completely removed (at fore-flap position 3).

No scale-effect tests were made because the results of earlier tests of the NACA 23021 airfoil with a slotted flap (reference 1) are considered applicable to the results of the present investigation.

An angle-of-attack range from -6° to the angle of attack for maximum lift was covered in 2° increments over most of the range for each test; however, when the stall condition was approached the increment was reduced to 1°. Very little data were obtained for angles of attack above the stall because of the unsteady condition of the model. Lift, drag, and pitching moment were measured at each angle of attack.

RESULTS AND DISCUSSION

Coefficients and Symbols

All the test results are given in standard section nondimensional coefficient form corrected for tunnel-wall effect and turbulence as explained in reference 6.

c_l section lift coefficient (l/qc)

c_{d_o} section profile-drag coefficient (d_o/qc)

$c_{m_{(a.c.)_o}}$ section pitching-moment coefficient about aerodynamic center of plain airfoil $\left[m_{(a.c.)_o}/qc^2\right]$ (fig. 2)

$\left[c_{m_{(a.c.)_o}}\right]_{c_{l_{max}}}$ section pitching-moment coefficient at maximum section lift coefficient

$c_{l_{max}}$ maximum section lift coefficient

$c_{d_{o_{min}}}$ minimum section profile-drag coefficient

where

l section lift

d_o section profile drag

$m_{(a.c.)_o}$ section pitching moment about aerodynamic center of plain airfoil (fig. 2)

q dynamic pressure $\left(\frac{1}{2}\rho V^2\right)$

c chord of basic airfoil with flap fully retracted

V velocity, feet per second

ρ mass density of air

and

R_e effective Reynolds number

l_t distance from aerodynamic center of airfoil to center of pressure of tail, expressed in airfoil chords

α_o angle of attack for infinite aspect ratio

δ_{f_1} fore-flap deflection, measured between fore-flap chord and airfoil chord

δ_{f_2} rear-flap deflection, measured between rear-flap chord and airfoil chord

x_1 distance from airfoil upper-surface lip to fore-flap-nose point, measured parallel to airfoil chord and positive when fore-flap-nose point is ahead of lip

y_1 distance from airfoil upper-surface lip to fore-flap-nose point, measured perpendicular to airfoil chord and positive when fore-flap-nose point is below lip

x_2 distance from fore-flap trailing edge to rear-flap-nose point, measured parallel to airfoil chord and positive when rear-flap-nose point is ahead of fore-flap trailing edge

y_2 distance from fore-flap trailing edge to rear-flap-nose point, measured perpendicular to airfoil chord and positive when rear-flap-nose point is below fore-flap trailing edge

Precision

The accuracy of the various measurements in the tests is believed to be within the following limits:

α_o, degrees	± 0.1
$c_{l_{max}}$	± 0.03
$c_{m(a.c.)_o}$	± 0.003
$c_{d_{o_{min}}}$	± 0.0003
$c_{d_{o(c_l = 1.0)}}$	± 0.0006
$c_{d_{o(c_l = 2.5)}}$	± 0.002
δ_{f_1} and δ_{f_2}, degrees	± 0.2
Flap position	$\pm 0.001c$

No corrections were determined (or applied) for the effect of the airfoil or flap fittings on the section aerodynamic characteristics because of the large number of tests required. It is believed, however, that their effect is small and that the relative values of the results would not be appreciably affected.

Plain Airfoil

The complete aerodynamic section characteristics of the plain NACA 23021 airfoil (from reference 1) are presented in figure 2. Since these data have already been discussed in reference 1, no further comment is believed necessary.

Determination of Optimum Flap Configurations

Maximum lift.- The results of the maximum-lift investigation with the fore flap at each of the three selected positions and with the rear flap deflected and located at points over a considerable area with respect to the fore flap are presented in figures 3 to 5. The results are presented as contours of lift coefficient for various positions of the rear-flap-nose point at various rear-flap deflections. The results show that at each fore-flap position, the contours did not close at the smaller rear-flap deflections investigated. At positions 1 and 2, it is indicated that the open contours would close at positions of the rear-flap nose that would be impracticable because of the large gap between the two flaps.

At each of the three fore-flap positions, as the flap deflection increased, the position of the rear flap for maximum section lift coefficient $c_{l_{max}}$ generally became more critical - that is, a given movement of the rear-flap-nose point caused a greater change in the value of $c_{l_{max}}$. Since the position of the rear-flap nose for $c_{l_{max}}$ tends to move forward and upward as its deflection increases, the gap between the two flaps is reduced. The values of $c_{l_{max}}$ obtained at each fore-flap position and the approximate position of the rear-flap nose with respect to the fore-flap trailing edge are given in the following table:

Fore-flap position	Position of rear-flap nose: Ahead of lip (percent airfoil chord)	Position of rear-flap nose: Below lip (percent airfoil chord)	$c_{l_{max}}$
1	1	6	2.71
2	0	2	3.06
3	2	3	3.31

From the contours of rear-flap-nose position for $c_{l_{max}}$, the best path to be followed by the rear flap at all deflections within the range investigated, from a consideration of $c_{l_{max}}$ alone, can be determined. The range of flap positions covered was considered sufficient to allow for any deviations or compromises from the best path. Complete aerodynamic section characteristics for the optimum-lift and optimum-drag rear-flap-nose positions at each selected fore-flap position are presented subsequently herein.

Minimum profile drag.- Drag data obtained with the fore flap in the three selected positions and the rear flap deflected at various positions over a wide region are presented in figures 6 to 8. The data are presented as drag contours for the rear-flap-nose position at certain selected section lift coefficients and rear-flap deflections. A comparison of the section profile-drag characteristics of the plain airfoil (fig. 2) with the profile-drag characteristics given in the contours of figure 6(a) and 6(b) shows that the plain airfoil gives the lower drag value at $c_l = 1.0$.

Inasmuch as only a very few of the contours were closed about indicated optimum-drag positions of the rear-flap nose (figs. 6 to 8), it is obvious that a sufficient range of rear-flap position was not covered and that the true optimum values may exist at some other positions. At each of the fore-flap positions, however, it is indicated that the contours would close at positions of the rear-flap nose which would be somewhat closer to the lip of the fore flap than the positions tested. As the fore flap was extended and as the rear flap was deflected, the optimum-drag rear-flap-nose position generally moved forward and up, closer to the fore-flap trailing edge. More than one region of minimum drag exists at various values of section lift coefficient c_l and various rear-flap deflections and the minimum drag is seen to be principally a function of section lift coefficient and rear-flap deflection and relatively independent of the fore-flap position. In each position of the fore flap, as the section lift coefficient or the rear-flap deflection increased, the contours generally became more critical or closely spaced; that is, a given movement of the rear-flap-nose point generally caused a greater change in the value of the section profile-drag coefficient c_{d_o}. (See figs. 6 to 8.)

Inasmuch as the rear-flap-nose positions for maximum lift and minimum drag generally do not coincide, a compromise is necessary. The curves for the complete aerodynamic section characteristics are therefore presented for both conditions.

Pitching moment.- Contours of section pitching-moment coefficient for the rear-flap-nose positions at selected section lift coefficients and rear-flap deflections are given for each of the three fore-flap positions in figures 9 to 11. These contours indicate that an increase in the negative value of $c_{m_{(a.c.)_o}}$ at a given c_l was obtained with increased rear-flap deflection and that the maximum negative values of $c_{m_{(a.c.)_o}}$ were usually obtained at or near the position of the rear-flap-nose point for maximum lift at each rear-flap deflection (compare with figs. 3 to 5). At $\delta_{f_2} = 50^\circ$, 60°, and 70° at position 3, however, a decrease in the value of $c_{m_{(a.c.)_o}}$ was indicated when c_l increased.

At a given lift coefficient and rear-flap deflection, the negative values of pitching moment also increased as the fore flap was extended from position 1 to position 3. It appears desirable therefore to use the minimum flap deflection or extension necessary to obtain any given lift coefficient. In addition, the contours indicate that the position of the rear-flap nose becomes more critical with increased rear-flap deflection and lift coefficient.

With these contours of flap location for $c_{m_{(a.c.)_o}}$ in figures 9 to 11, the designer can determine or anticipate the values of $c_{m_{(a.c.)_o}}$ to be encountered at a given value of c_l within the range of position and deflection indicated.

Aerodynamic Section Characteristics of Selected Optimum Configurations

The complete aerodynamic section characteristics of the airfoil with the rear flap at the optimum-lift and optimum-drag positions at each flap deflection and at each of the three fore-flap positions are presented in figures 12 to 14. The consecutive flap-nose positions as δ_{f_2} increases are indicated in the figures by those key symbols that are connected by dashed lines. The lift-curve slopes decreased with increased rear-flap deflection, although at rear-flap deflections below 50°, the lift-curve slope was sometimes as much as 0.03 greater than that of the plain airfoil. At each fore-flap position, the angle of attack for maximum lift usually decreased with increased rear-flap deflection but in some instances remained fairly constant.

At position 3 (fig. 14) and $\delta_{f_2} = 50^{\circ}$, the position of the rear flap for maximum lift and minimum drag coincide. Irregularities in the curves at the larger flap deflections (figs. 12 to 14) indicate changing flow conditions.

At the small rear-flap deflections and lift coefficients, the slopes of the pitching-moment curves were negative and, at high flap deflections and lift coefficients, were usually positive; smaller negative values of $c_{m_{(a.c.)_o}}$ were therefore sometimes obtained with a large flap deflection than with a small one at high lift coefficients. (See figs. 13 and 14.)

Increment of maximum section lift coefficient.- The increment of the maximum section lift coefficient $\Delta c_{l_{max}}$, based on the value of $c_{l_{max}}$ of the plain airfoil, increases as the rear flap is deflected and as the fore flap is extended (fig. 15). At each fore-flap position, the values of $\Delta c_{l_{max}}$ are higher for the optimum-lift position than for the optimum-drag rear-flap position, as was anticipated.

The maximum increment of lift coefficient obtained was at position 3 with $\delta_{f_2} = 70^{\circ}$, where a value of 1.96 is indicated. The scale effect on the values of $\Delta c_{l_{max}}$ was not investigated but it is expected that the values would increase slightly with Reynolds number with the 0.32c double slotted flap as did the values for the single-slotted-flap arrangements of references 1 and 6.

Envelope polar curves.- The envelope polars of section profile-drag coefficient c_{d_o} at each fore-flap position, obtained from figures 12 to 14 for the optimum-lift and optimum-drag configurations, and the polar of the plain airfoil are presented in figure 16. These curves indicate the $c_{d_{o_{min}}}$ available at any c_l when the rear flap is located to give $c_{l_{max}}$ (fig. 16(a)) and $c_{d_{o_{min}}}$ (fig. 16(b)).

For both the maximum-lift and minimum-drag configurations (fig. 16), the plain airfoil gives the lowest c_{d_o} for values of c_l less than 1.3, and for values of c_l above 2.6 the lowest value of c_{d_o} is indicated at position 3.

Comparison of Flap Arrangements

When the lift-drag characteristics of the 0.2566c and 0.40c single slotted flaps (references 1 and 2) and the 0.40c double slotted flap (reference 3) are compared with those of the optimum-lift and optimum-drag configurations of the 0.32c double slotted flap (fig. 17), it is apparent that the 0.40c double-slotted-flap arrangement produced the highest lift coefficient ($c_l = 3.56$) on the NACA 23021 airfoil. The $c_{l_{max}}$ obtained with the 0.32c double slotted flap is considerably higher than that obtained with either single slotted flap but it is approximately 0.25 less than that of the 0.40c double slotted flap.

The 0.32c double slotted flap had a larger c_{d_o} than either single slotted flap for values of c_l between 1.0 and approximately 2.7 and had a larger c_{d_o} than the 0.40c double-slotted-flap arrangement at all values of c_l above 1.0.

The 0.32c double-slotted-flap arrangement had values of c_{d_o} for the envelope polars that differed by about 0.02 for the optimum-drag and optimum-lift configurations at a value of c_l of about 2.5. At values of c_l less than 1.3 and greater than 3.1, however, the two polar curves practically coincide.

When the polars of the 0.32c double-slotted-flap arrangement on the NACA 23021 airfoil are compared with a similar arrangement of a 0.30c double slotted flap on the NACA 23012 airfoil (reference 4), it is apparent that the $c_{l_{max}}$ obtained with each is approximately the same (fig. 18). The values of c_{d_0}, however, are higher at all values of c_l for the arrangement on the 21-percent-thick airfoil than for that on the 12-percent-thick airfoil but the relation between optimum-lift and optimum-drag configurations is about the same for each arrangement.

A further comparison of the various slotted-flap arrangements on the NACA 23021 airfoil indicates that a fairly linear variation exists for each arrangement at a given flap configuration between the $c_{l_{max}}$ and the $\left[c_{m_{(a.c.)_0}}\right]_{c_{l_{max}}}$ (fig. 19) and this variation appears dependent on the flap arrangement. The 0.32c double slotted flap gave higher values of $\left[c_{m_{(a.c.)_0}}\right]_{c_{l_{max}}}$ at any value of c_l than any of the slotted flaps.

Inasmuch as there will be a tail load required to trim the negative pitching moment of the wing of an airplane, the loss in maximum section lift coefficient in trimming the airfoil section pitching-moment coefficient has been calculated, for the case when the center of gravity is at the aerodynamic center of the plain airfoil, from the following expression and is indicated in figure 19:

$$\text{Loss of } c_{l_{max}} = \frac{\left[c_{m_{(a.c.)_0}}\right]_{c_{l_{max}}}}{l_t}$$

The loss in $c_{l_{max}}$ has been presented for tail lengths of 2, 3, and 5 airfoil-chord lengths and, by means of the curves of figure 19, the effective $c_{l_{max}}$ can be determined.

Effect of Various Modifications on the Aerodynamic Section Characteristics

Effect of moving the two flaps as a unit.- The effect on the aerodynamic section characteristics of moving the fore flap and rear flap as a unit perpendicular and parallel to the airfoil chord is shown in figures 20 and 21, respectively. A 0.01c displacement downward of the flaps, perpendicular to the chord, was quite critical in that a large decrease in lift and an increase in drag resulted (fig. 20). Figure 21 indicates that a movement of the flaps parallel to the airfoil chord had a considerable effect on the aerodynamic characteristics; that is, at positions of the fore flap downstream from $x_1 = 0.70$ (position 3), large decreases in lift and increases in drag resulted and unsteady flow conditions existed. A comparison of figures 20 and 21 with the contours of figures 4 and 7 and 5 and 8, respectively, indicates that the position of the fore flap is more critical than the position of the rear flap.

Moving the two flaps approximately as a unit from position 1 to position 2 and then to position 3 along two different paths, A and B, gave an increase in lift, drag, and pitching moment. (See figs. 22 and 23.) Since the model fittings only allowed increments of 10° for the deflection of the rear flap, it was not possible to have a δ_{f_2} of 35° for figure 22 and a δ_{f_2} of 45° for figure 23 at position 1. Although motion of the two flaps as a unit is only approximately simulated, figures 22 and 23 are thought to be sufficiently illustrative.

Effect of the airfoil lower lip.- The effects of deflecting the lower lip of the airfoil from its normal position at fore-flap position 2 and of removing the lower airfoil lip at position 3 are shown in figures 24 and 25, respectively. Deflecting the lip upward 19° decreased c_l and increased c_{d_o} over most of the angle-of-attack range, possibly because of the poorly shaped slot entry ahead of the fore flap when the lip is deflected. On the other hand, removing the lip at the extended fore-flap position (fig. 25) had a slightly favorable effect on the aerodynamic section characteristics at low values of c_l, by causing a reduction in the profile drag, and a slightly adverse effect at high values of c_l. Such a result indicates that a smoother slot entry ahead of the flaps may be desirable, provided it does not reduce the values of $c_{l_{max}}$ available. Although no data were obtained at small flap deflections, it is probable that the smoother slot entry would be even more favorable under such conditions.

CONCLUSIONS

An investigation was made in the LMAL 7- by 10-foot tunnel of an NACA 23021 airfoil with a double slotted flap having a chord 32 percent of the airfoil chord (0.32c) to determine the aerodynamic section characteristics with the flaps deflected at various positions. The results of this investigation show that:

1. The 0.32c double slotted flap on the NACA 23021 airfoil gave a maximum section lift coefficient of 3.31, which was larger than the value obtained with the 0.2566c or 0.40c single slotted flaps and 0.25 less than the value obtained with the 0.40c double slotted flap on the same airfoil.

2. The values of the profile-drag coefficient obtained with the 0.32c double slotted flap were larger than those for the 0.2566c or 0.40c single slotted flaps for section lift coefficients between 1.0 and approximately 2.7. At all values of the section lift coefficient above 1.0, the present arrangement had a higher profile drag than the 0.40c double slotted flap.

3. At a given value of the maximum section lift coefficient produced by various flap deflections, the 0.32c double slotted flap gave negative section pitching-moment coefficients that were higher than those of other slotted flaps on the same airfoil.

4. The 0.32c double slotted flap gave approximately the same maximum lift coefficient as, but higher profile-drag coefficient over the entire lift range than, a similar arrangement of a 0.30c double slotted flap on an NACA 23012 airfoil.

5. Moving the flaps slightly from their optimum positions sometimes proved critical and resulted in a

large increase in drag and a reduction in lift. The position of the fore flap appears to be more critical than that of the rear flap.

6. Deflecting the lower lip of the airfoil 19° upward generally decreased the section lift coefficient and increased the section profile-drag coefficient over most of the angle-of-attack range; removing the lip at the extended fore-flap position reduced the profile drag slightly in the lower-lift range but was slightly unfavorable at high section lift coefficients.

Langley Memorial Aeronautical Laboratory
National Advisory Committee for Aeronautics
Langley Field, Va.

REFERENCES

1. Wenzinger, Carl J., and Harris, Thomas A.: Wind-Tunnel Investigation of an N.A.C.A. 23021 Airfoil with Various Arrangements of Slotted Flaps. NACA Rep. No. 677, 1939.

2. Duschik, Frank: Wind-Tunnel Investigation of an N.A.C.A. 23021 Airfoil with Two Arrangements of a 40-Percent-Chord Slotted Flap. NACA TN No. 728, 1939.

3. Harris, Thomas A., and Recant, Isidore G.: Wind-Tunnel Investigation of NACA 23012, 23021, and 23030 Airfoils Equipped with 40-Percent-Chord Double Slotted Flaps. NACA Rep. No. 723, 1941.

4. Purser, Paul E., Fischel, Jack, and Riebe, John M.: Wind-Tunnel Investigation of an NACA 23012 Airfoil with a 0.30-Airfoil-Chord Double Slotted Flap. NACA ARR No. 3L10, 1943.

5. Harris, Thomas A.: The 7 by 10 Foot Wind Tunnel of the National Advisory Committee for Aeronautics. NACA Rep. No. 412, 1931.

6. Wenzinger, Carl J., and Harris, Thomas A.: Wind-Tunnel Investigation of an N.A.C.A. 23012 Airfoil with Various Arrangements of Slotted Flaps. NACA Rep. No. 664, 1939.

7. Jacobs, Eastman N., and Sherman, Albert: Airfoil Section Characteristics as Affected by Variations of the Reynolds Number. NACA Rep. No. 586, 1937.

TABLE I

ORDINATES FOR AIRFOIL AND FLAPS

[Stations and ordinates in percent of airfoil chord]

NACA 23021 airfoil			Fore flap			Rear flap		
Station	Upper surface	Lower surface	Station	Upper surface	Lower surface	Station	Upper surface	Lower surface
0	-----	0	0	0	0	0	-0.55	-0.55
1.25	4.87	-2.08	1.39	1.72	-1.75	.32	.59	-1.81
2.5	6.14	-3.14	2.78	2.11	-1.97	.64	1.08	-2.30
5	7.93	-4.52	4.17	2.28	-1.78	1.28	1.89	-2.88
7.5	9.13	-5.55	5.56	2.30	-1.22	1.93	2.44	-3.28
10	10.03	-6.32	6.94	2.14	-.528	2.57	2.88	-3.53
15	11.19	-7.51	8.33	1.92	.222	5.14	3.96	-3.91
20	11.80	-8.30	9.72	1.61	.667	7.70	4.26	-3.79
25	12.05	-8.76	11.11	1.25	.722	10.27	3.99	-3.34
30	12.06	-8.95	12.50	.806	.50	12.83	3.42	-2.84
40	11.49	-8.83	13.89	.306	.167	15.40	2.83	-2.36
50	10.40	-8.14	14.67	0	-.052	17.96	2.21	-1.86
60	8.90	-7.07				20.53	1.56	-1.35
70	7.09	-5.72				23.10	.90	-.81
80	5.05	-4.13				25.66	.22	-.22
90	2.76	-2.30						
95	1.53	-1.30						
100	.22	-.22						
L.E. radius: 4.85 Slope of radius through end of chord: 0.305			L.E. radius: 1.58 Center of L.E. radius located on chord line			L.E. radius: 2.89 Center of L.E. arc: Upper surface, 2.89 Lower surface, -0.55		

NATIONAL ADVISORY
COMMITTEE FOR AERONAUTICS

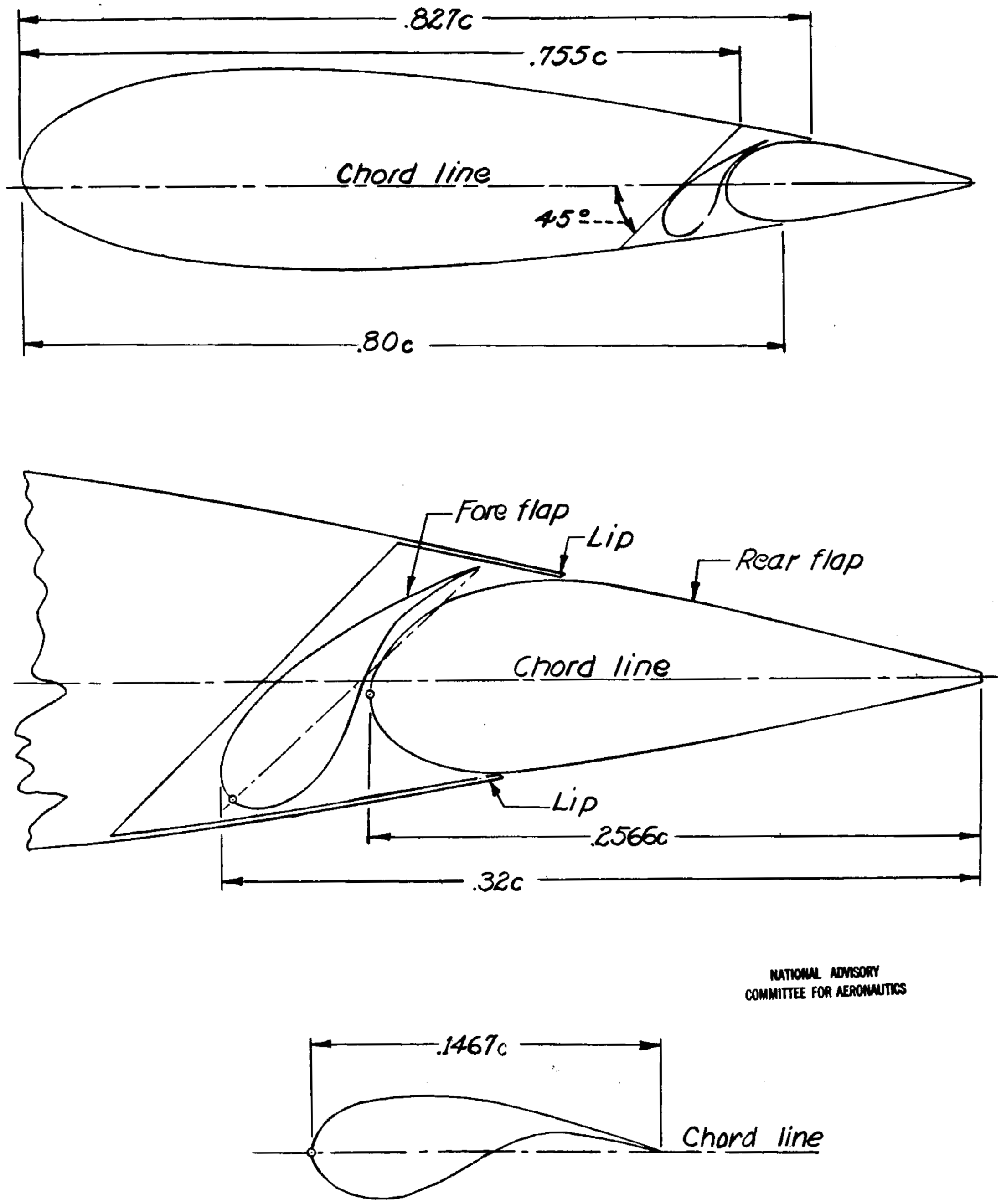

Figure 1.- Sections of the NACA 23021 airfoil and the 0.32c double slotted flap.

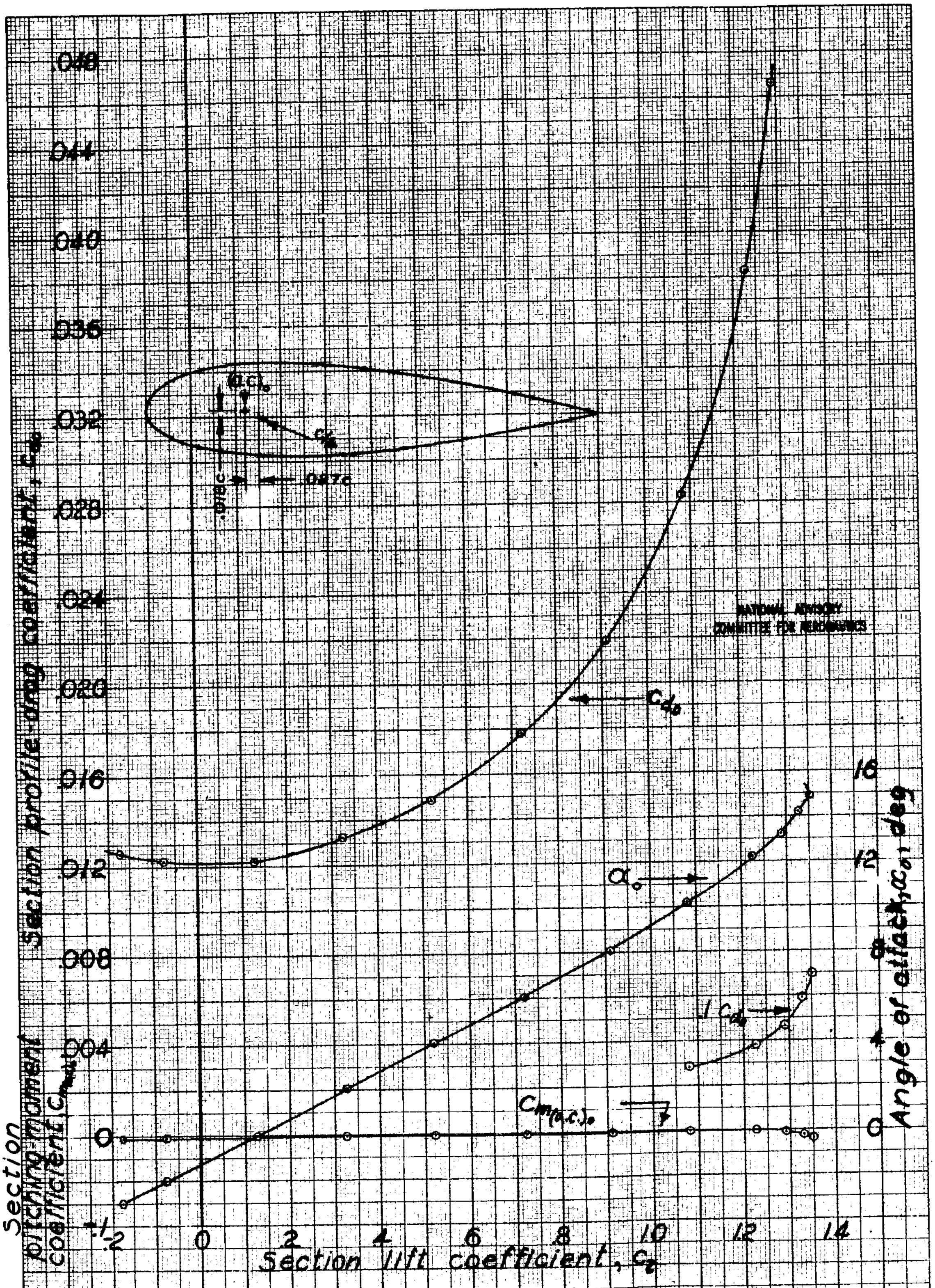

Figure 2.- Aerodynamic section characteristics of NACA 23021 plain airfoil. (From reference 1.)

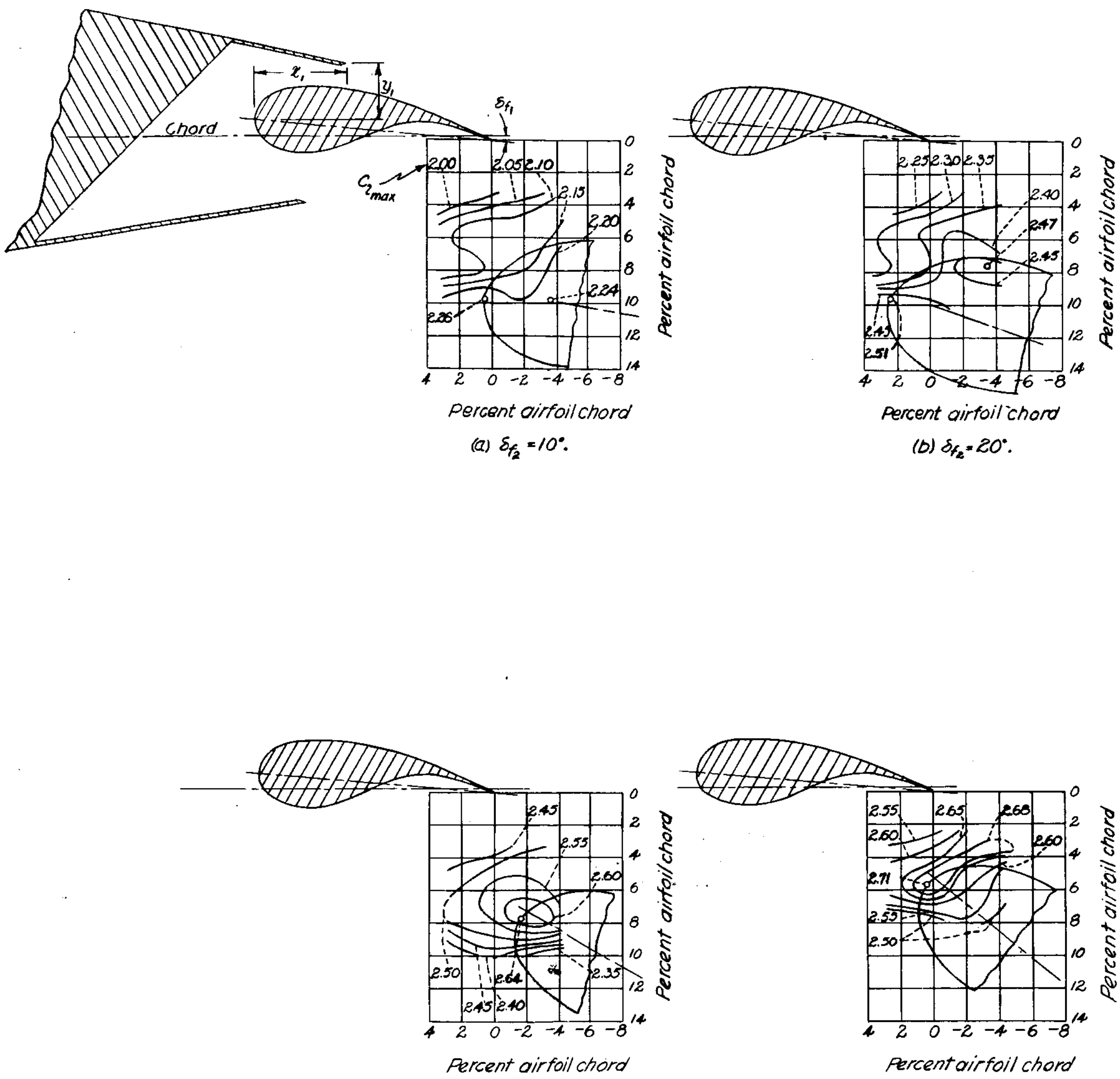

NATIONAL ADVISORY COMMITTEE FOR AERONAUTICS

Figure 3.- Contours of rear-flap position for $c_{l_{max}}$. Position 1; δ_{f_1}=5°; x_1=5.70; y_1=3.45. (Values of x_1, y_1 are given in percent airfoil chord.)

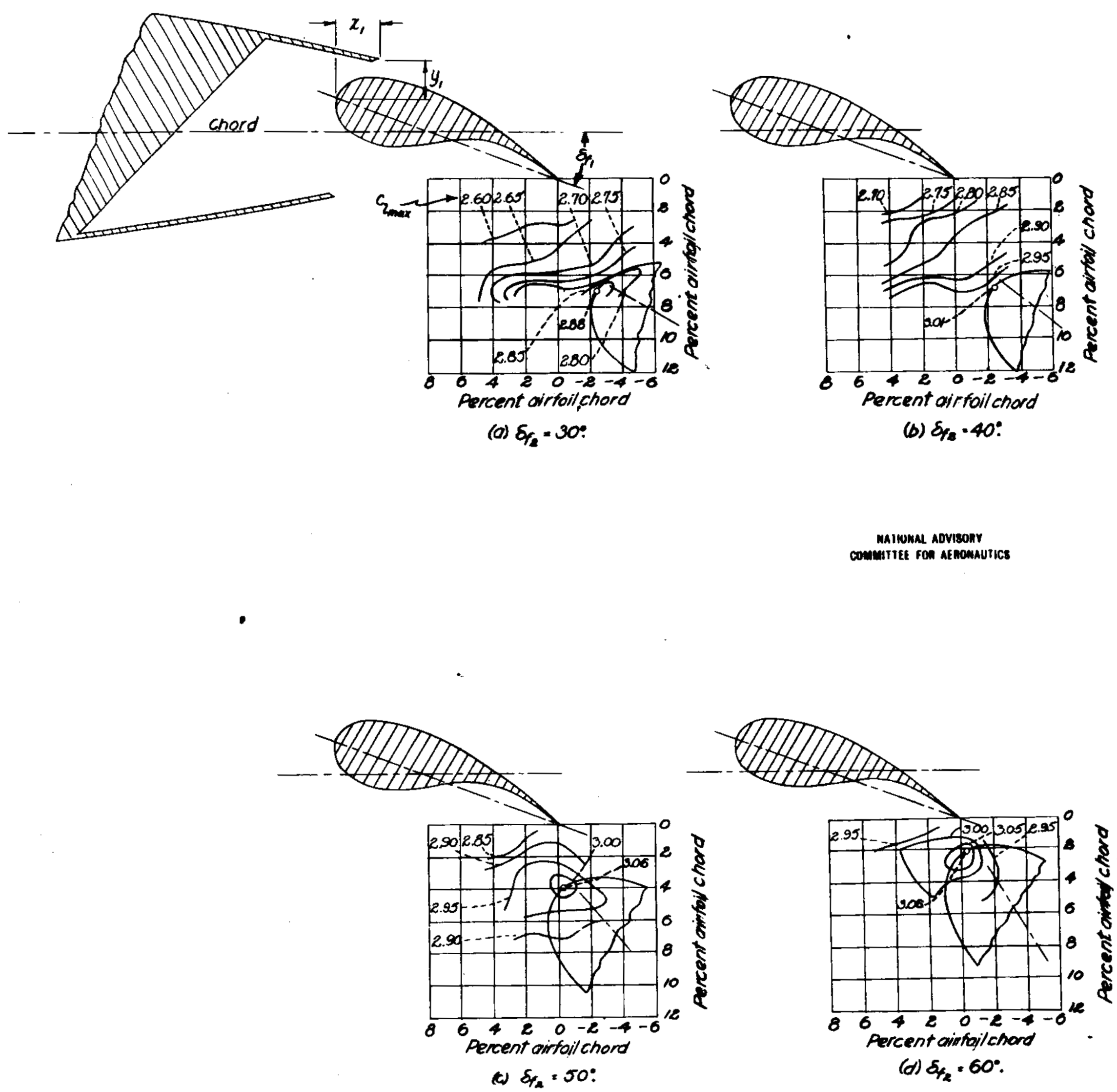

Figure 4.- Contours of rear-flap position for $c_{l_{max}}$. Position 2; δ_{f_1}=20°; x_1=2.70; y_1=2.45. (Values of x_1, y_1 are given in percent airfoil chord.)

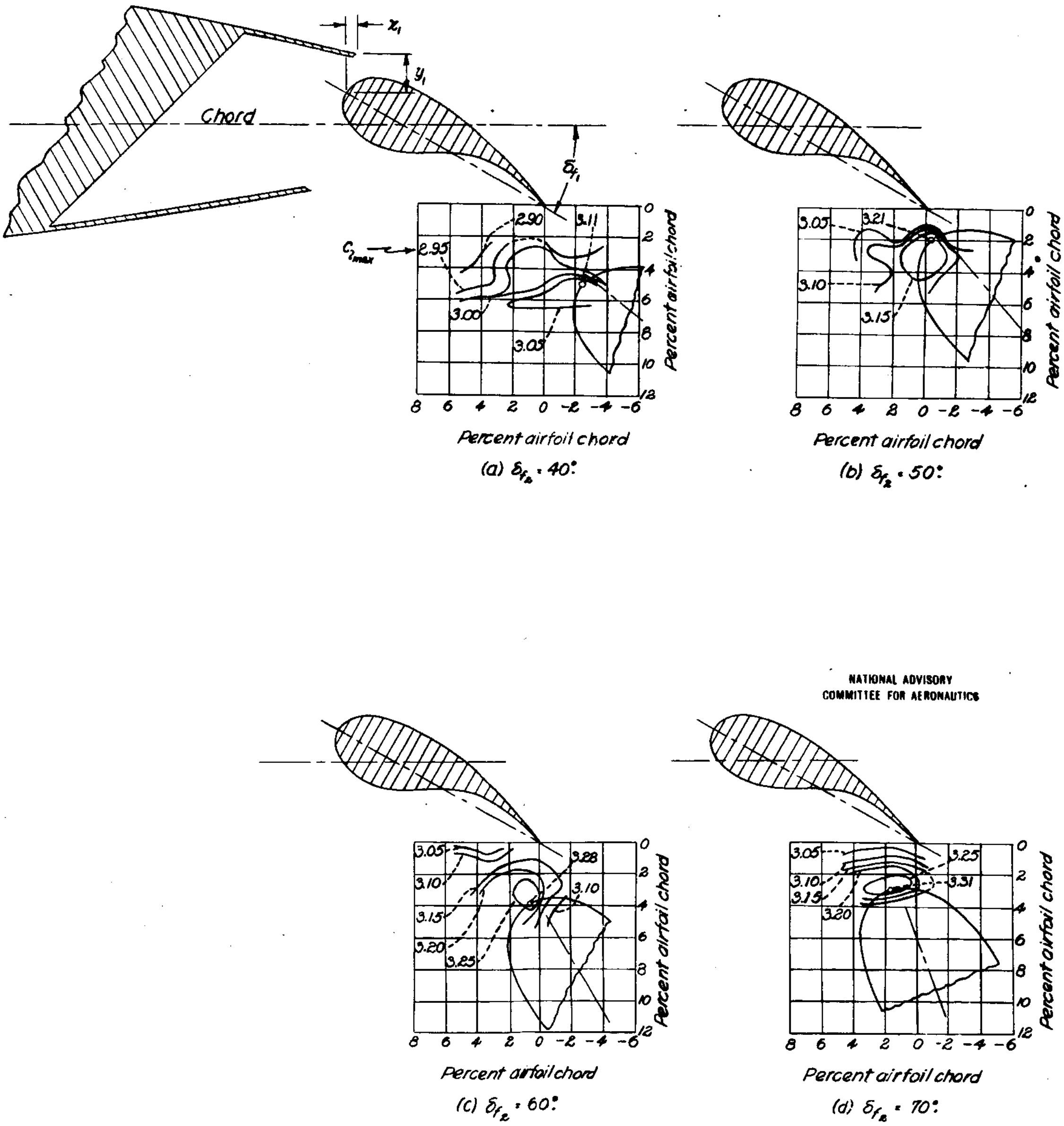

Figure 5.- Contours of rear-flap position for $c_{l_{max}}$. Position 3; $\delta_{f_1} = 30°$; $x_1 = 0.70$; $y_1 = 2.45$. (Values of x_1, y_1 are given in percent airfoil chord.)

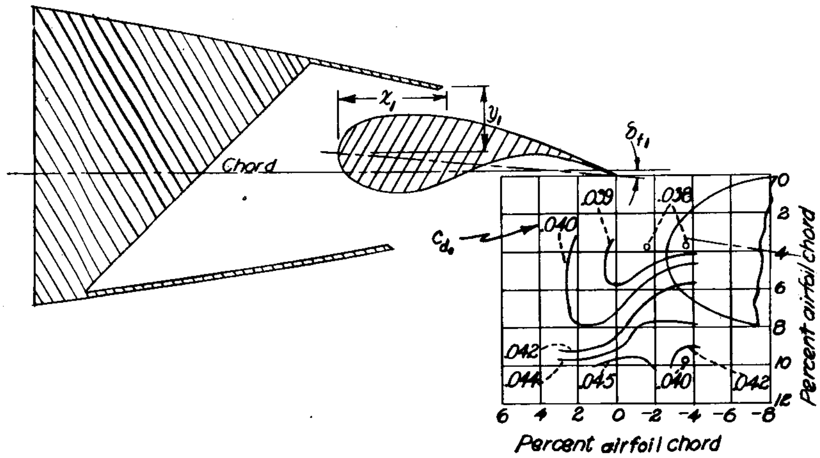

(a) $c_l = 1.0$; $\delta_{f_2} = 10°$.

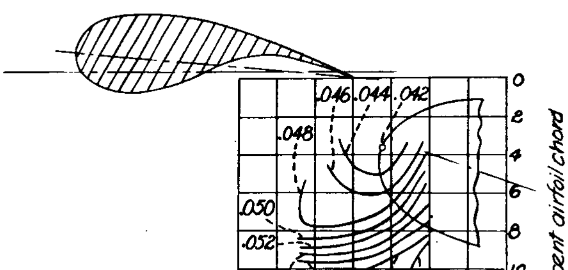

(b) $c_l = 1.0$; $\delta_{f_2} = 20°$.

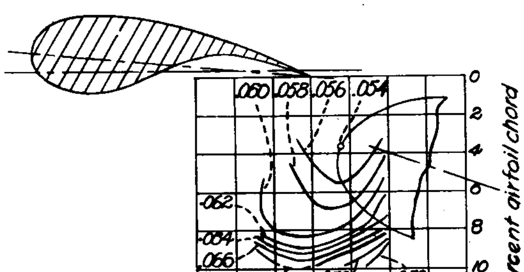

(c) $c_l = 1.5$; $\delta_{f_2} = 20°$.

Figure 6.- Contours of rear-flap position for c_{d_0}. Position 1; $\delta_{f_1} = 5°$; $x_1 = 5.70$; $y_1 = 3.45$. (Values of x_1, y_1 are given in percent airfoil chord.)

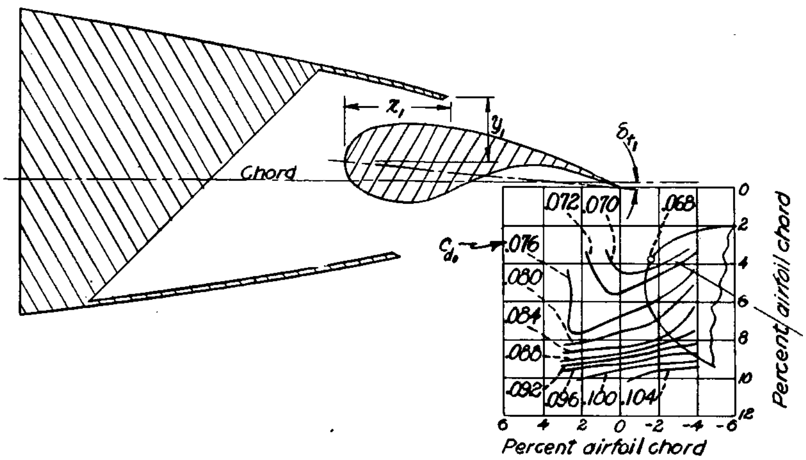

(d) $c_l = 1.5$; $\delta_{f_2} = 30°$.

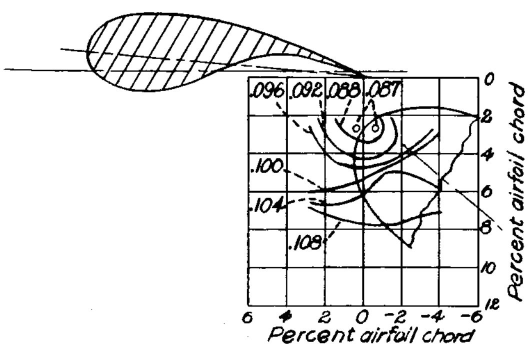

(e) $c_l = 1.5$; $\delta_{f_2} = 40°$.

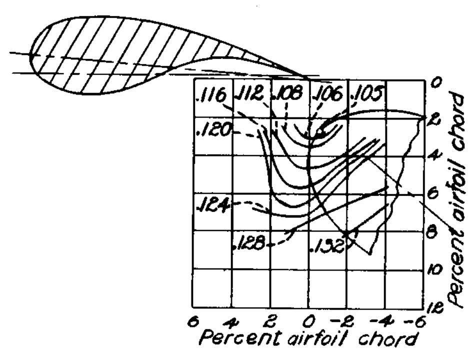

(f) $c_l = 2.0$; $\delta_{f_2} = 40°$.

Figure 6.- Concluded.

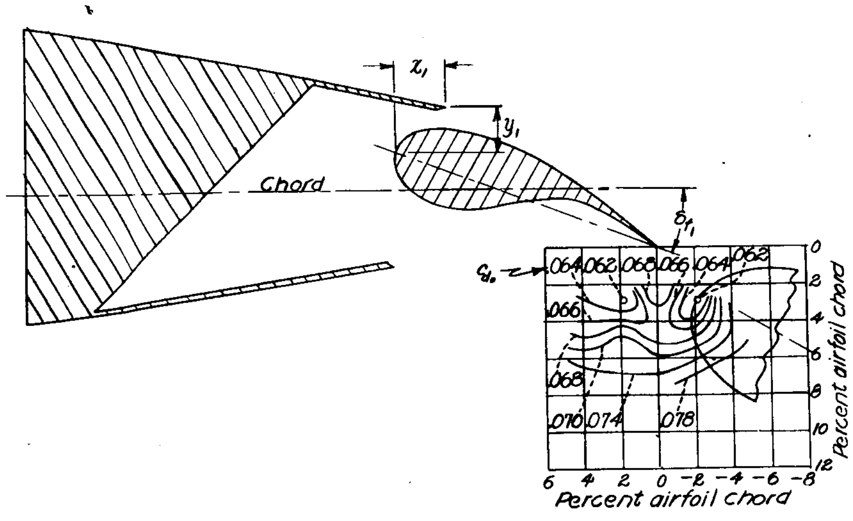

(a) $c_l = 1.5$; $\delta_{f_2} = 30°$.

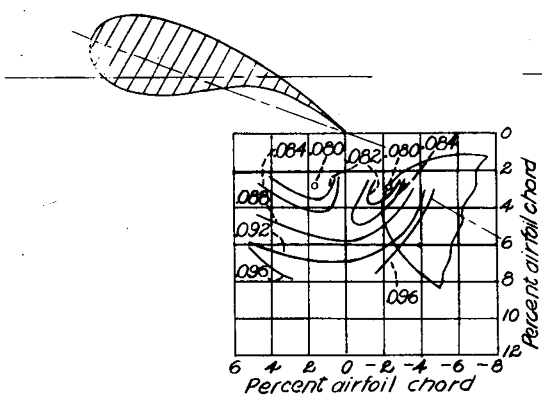

(b) $c_l = 2.0$; $\delta_{f_2} = 30°$.

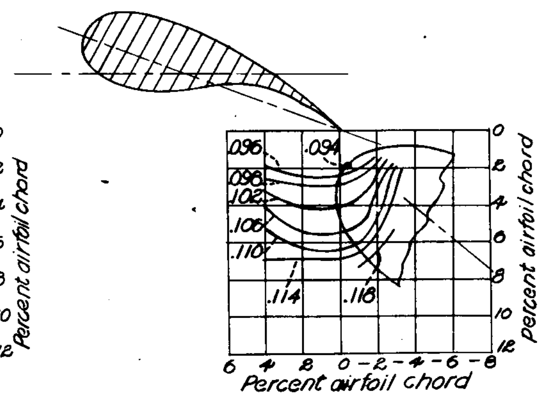

(c) $c_l = 2.0$; $\delta_{f_2} = 40°$.

Figure 7.- Contours of rear-flap position for c_{d_0}. Position 2; $\delta_{f_1} = 20°$; $x_1 = 2.70$; $y_1 = 2.45$. (Values of x_1, y_1 are given in percent airfoil chord.)

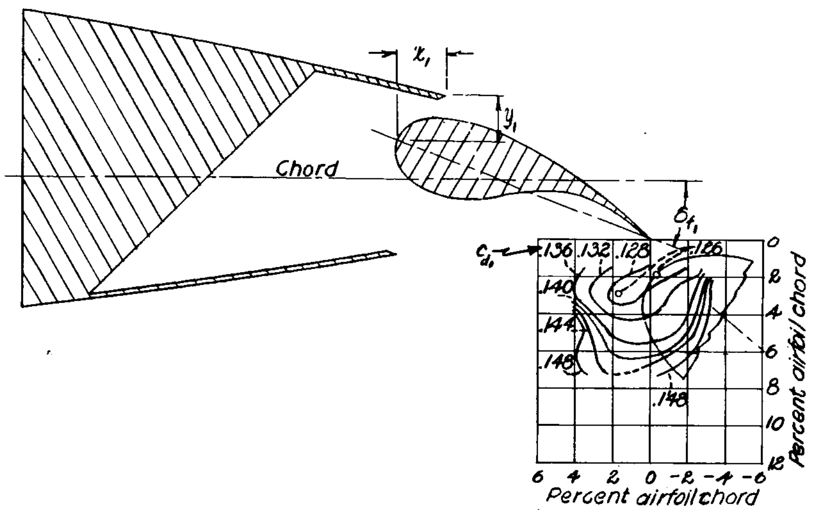

(d) $c_l = 2.5$; $\delta_{f_2} = 40°$.

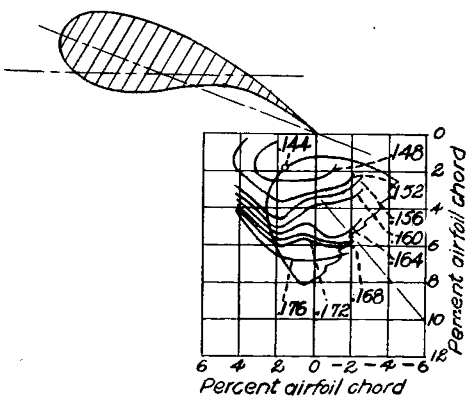

(e) $c_l = 2.5$; $\delta_{f_2} = 50°$.

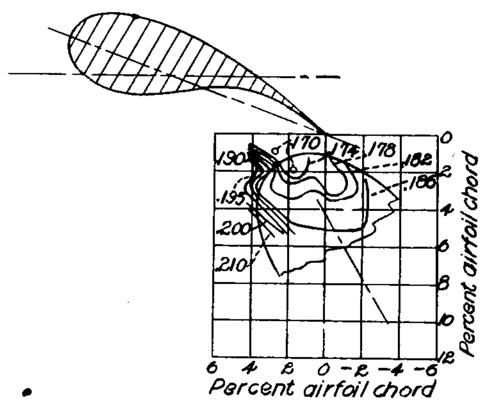

(f) $c_l = 2.5$; $\delta_{f_2} = 60°$.

Figure 7.- Concluded.

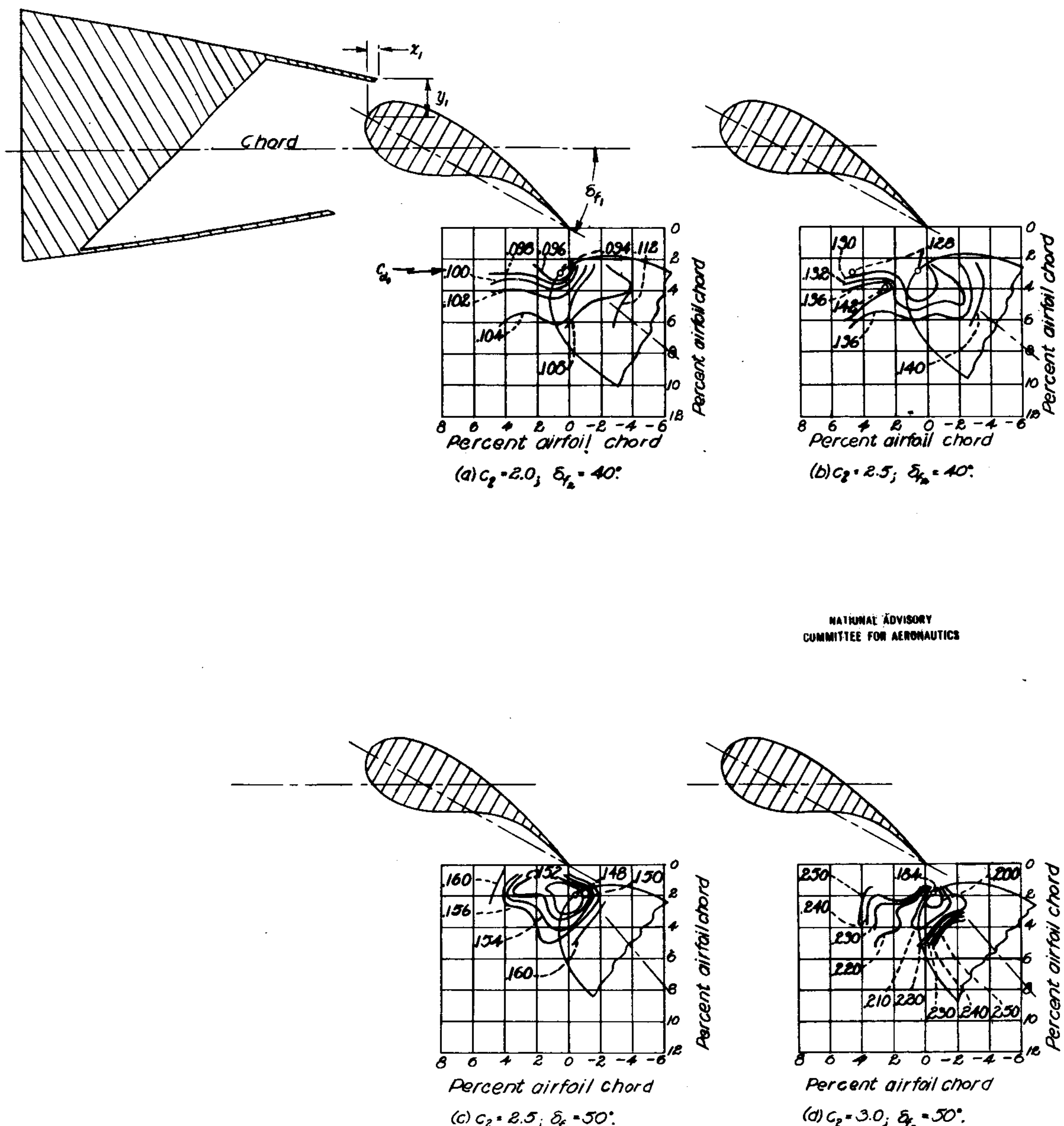

Figure 8.- Contours of rear-flap position for c_{d_o}. Position 3; δ_{f_1}=30°; x_1=0.70; y_1=2.45. (Values of x_1, y_1 are given in percent airfoil chord.)

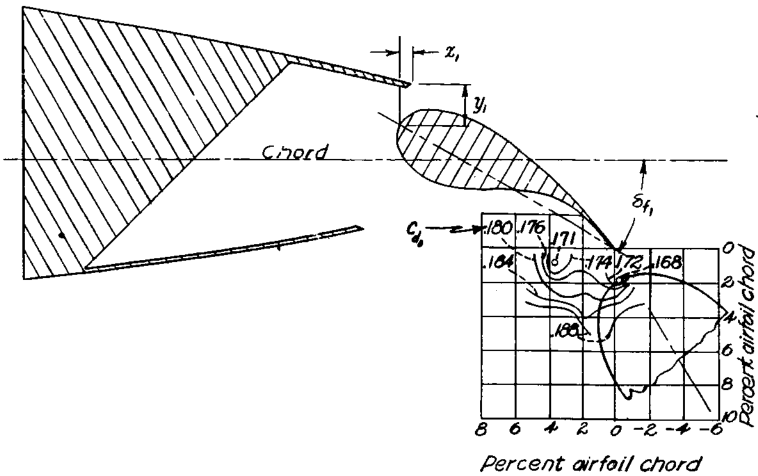

(e) $c_l = 2.5$; $\delta_{f_2} = 60°$.

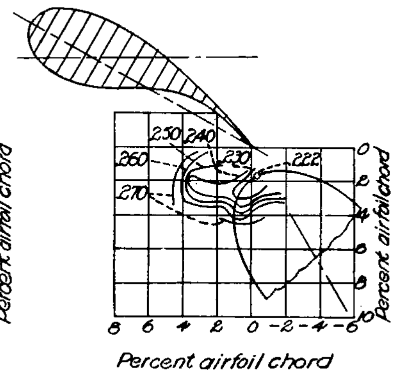

(f) $c_l = 3.0$; $\delta_{f_2} = 60°$.

NATIONAL ADVISORY
COMMITTEE FOR AERONAUTICS

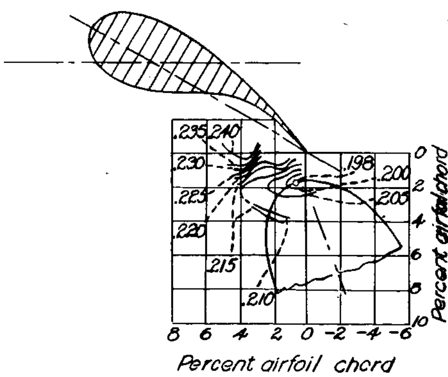

(g) $c_l = 2.5$; $\delta_{f_2} = 70°$.

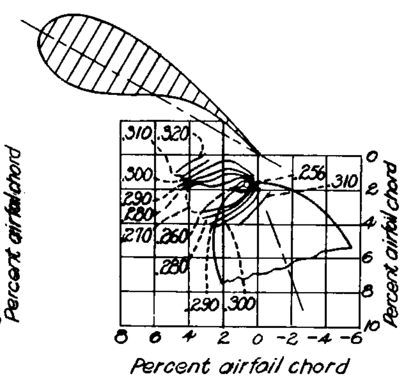

(h) $c_l = 3.0$; $\delta_{f_2} = 70°$.

Figure 8.- Concluded.

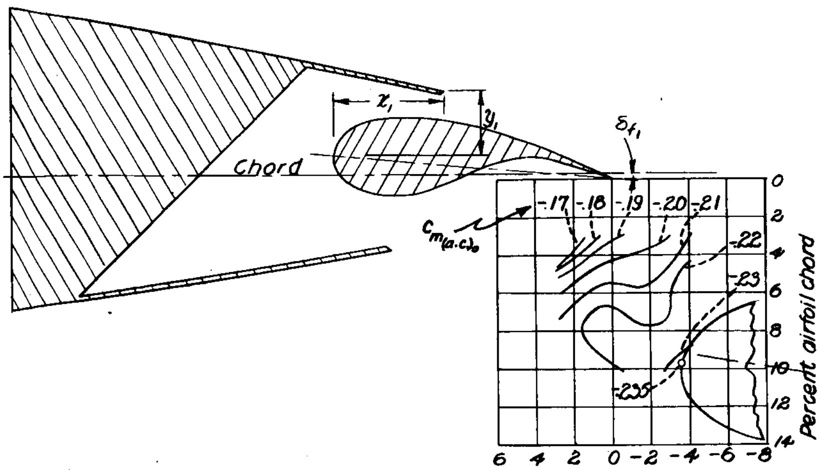

(a) $c_l = 1.0$; $\delta_{f_2} = 10°$.

NATIONAL ADVISORY COMMITTEE FOR AERONAUTICS

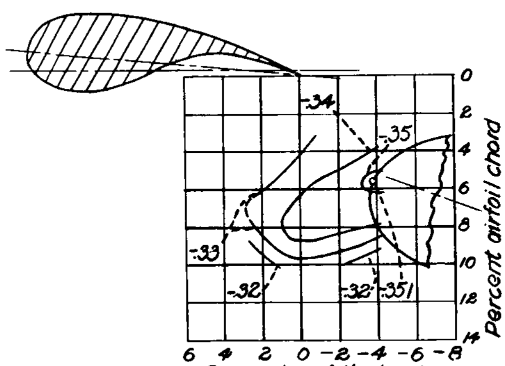

(b) $c_l = 1.0$; $\delta_{f_2} = 20°$.

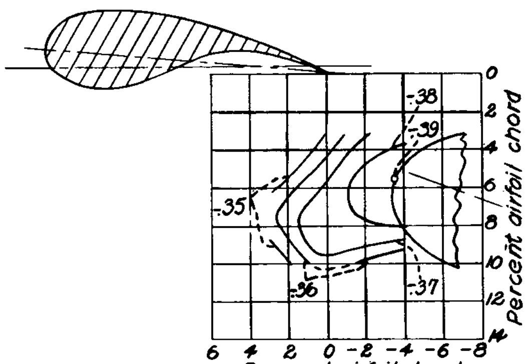

(c) $c_l = 1.5$; $\delta_{f_2} = 20°$.

Figure 9.- Contours of rear-flap position for $c_{m_{(a.c.)_0}}$. Position 1; $\delta_{f_1} = 5°$; $x_1 = 5.70$; $y_1 = 3.45$. (Values of x_1, y_1 are given in percent airfoil chord.)

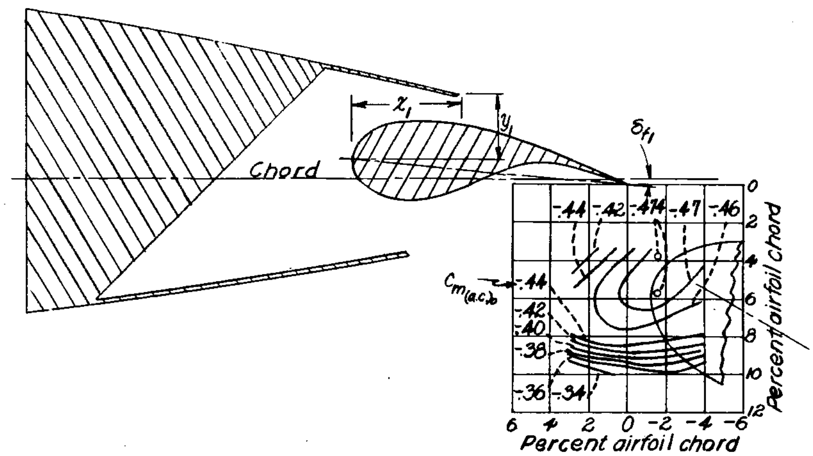

(d) $c_l = 1.5$; $\delta_{f_2} = 30°$.

NATIONAL ADVISORY
COMMITTEE FOR AERONAUTICS

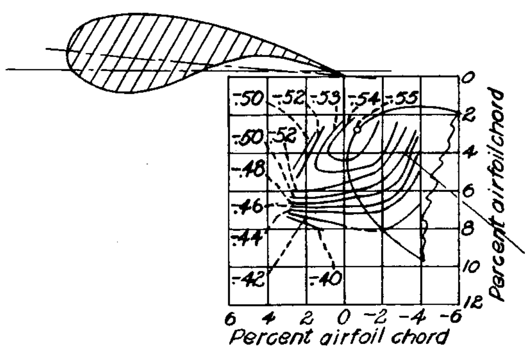

(e) $c_l = 1.5$; $\delta_{f_2} = 40°$.

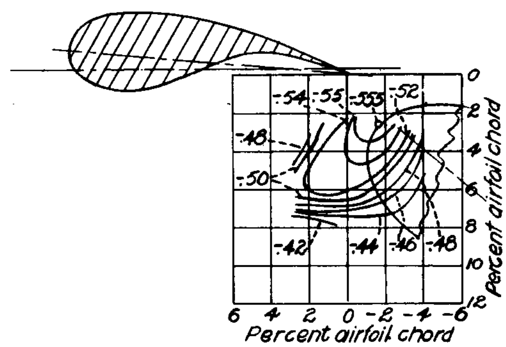

(f) $c_l = 2.0$; $\delta_{f_2} = 40°$.

Figure 9.- Concluded.

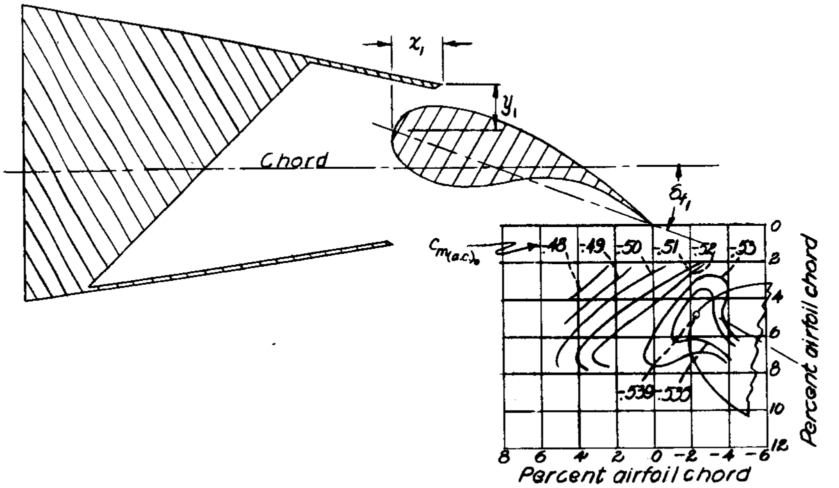

(a) $c_l = 1.5$; $\delta_{f_2} = 30°$.

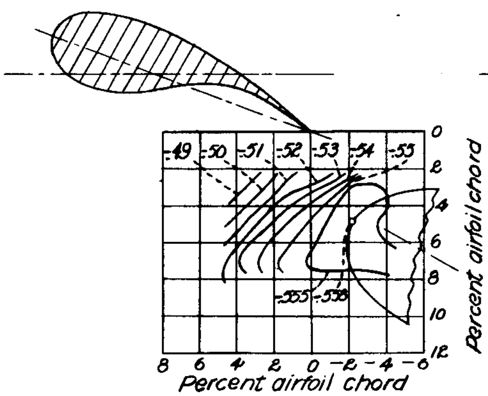

(b) $c_l = 2.0$; $\delta_{f_2} = 30°$.

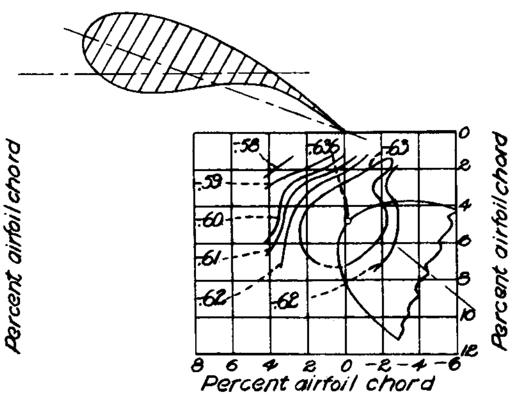

(c) $c_l = 2.0$; $\delta_{f_2} = 40°$.

Figure 10.- Contours of rear-flap position for $c_{m_{(a.c.)_0}}$. Position 2; $\delta_{f_1}=20°$; $x_1=2.70$; $y_1=2.45$. (Values of x_1, y_1 are given in percent airfoil chord.)

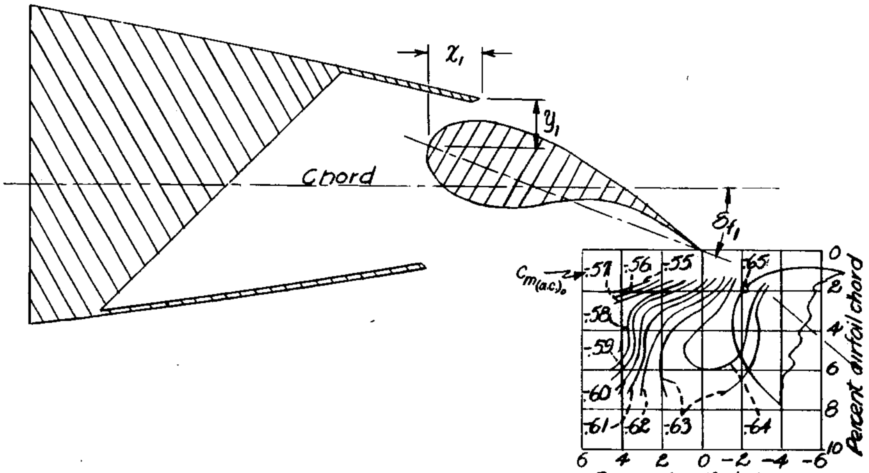

(d) $c_l = 2.5$; $\delta_{f_2} = 40°$.

NATIONAL ADVISORY
COMMITTEE FOR AERONAUTICS

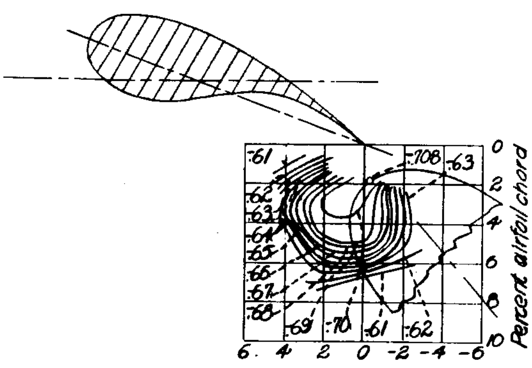

(e) $c_l = 2.5$; $\delta_{f_2} = 50°$.

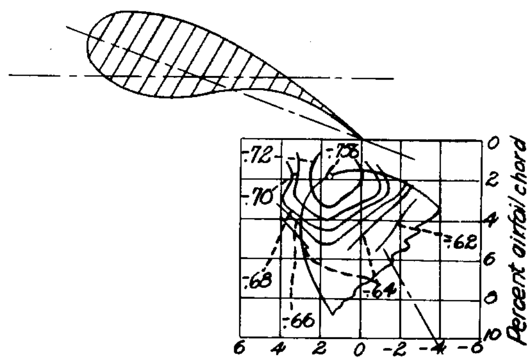

(f) $c_l = 2.5$; $\delta_{f_2} = 60°$.

Figure 10.- Concluded.

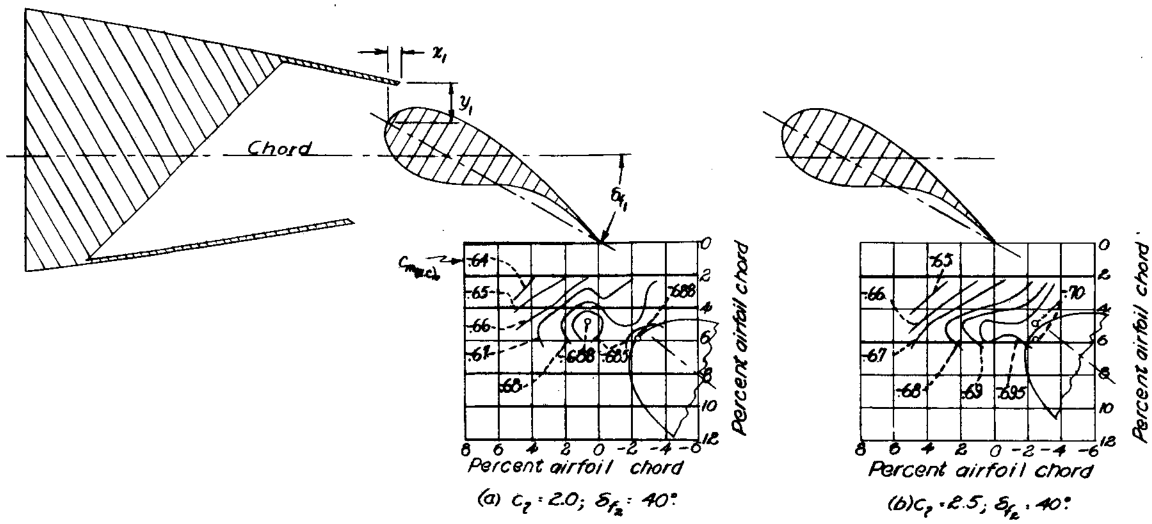

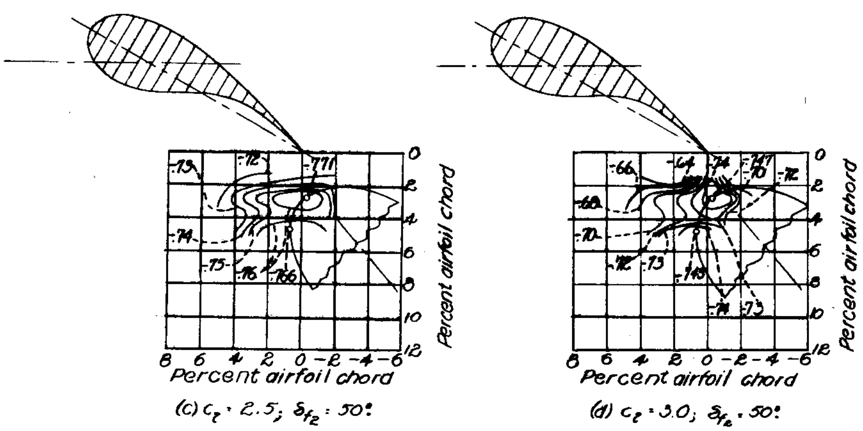

Figure 11.- Contours of rear-flap position for $c_{m(a.c.)_0}$. Position 3; $\delta_{f_1} = 30°$; $x_1 = 0.70$; $y_1 = 2.45$. (Values of x_1, y_1 are given in percent airfoil chord.)

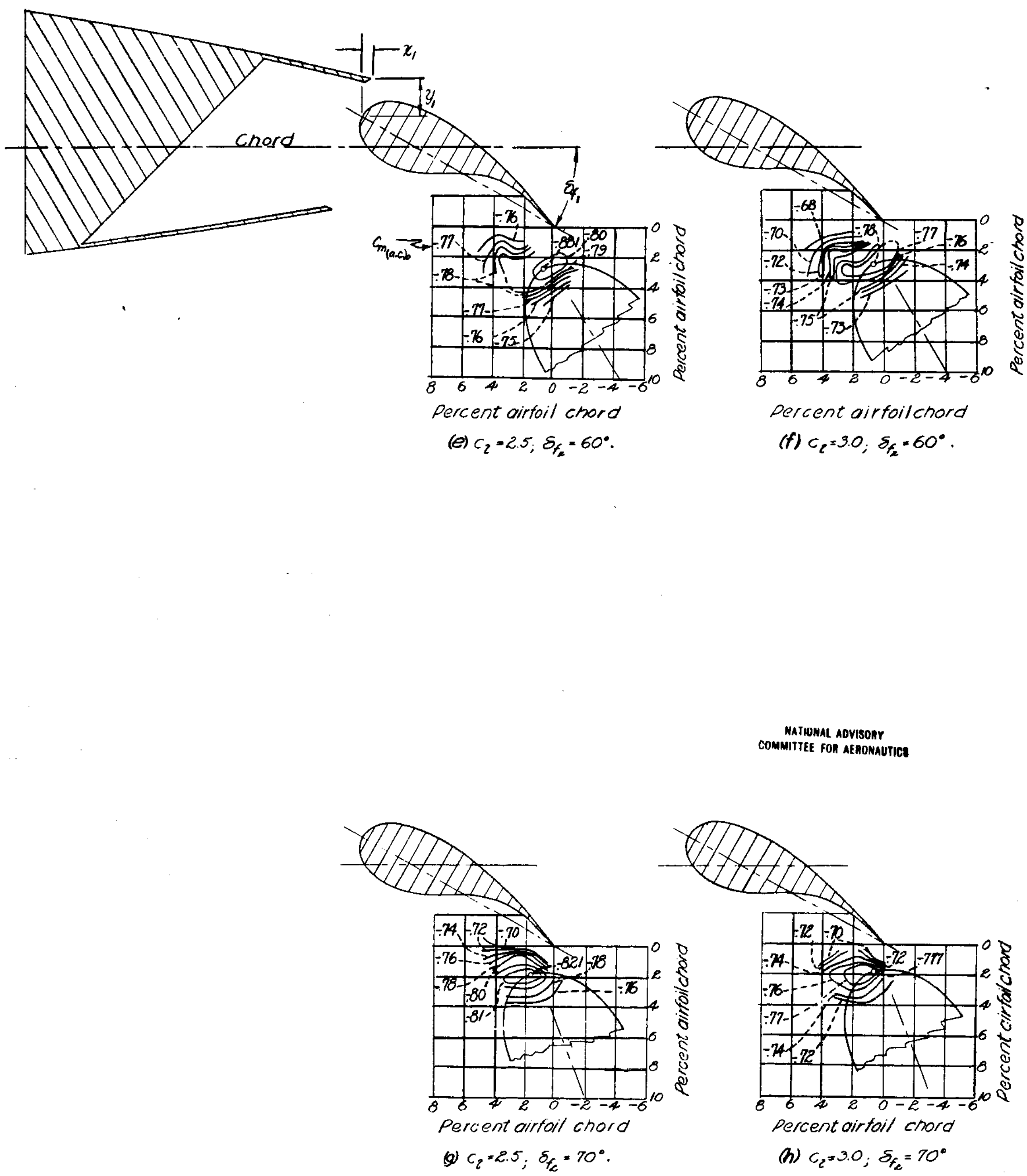

Figure 11.- Concluded.

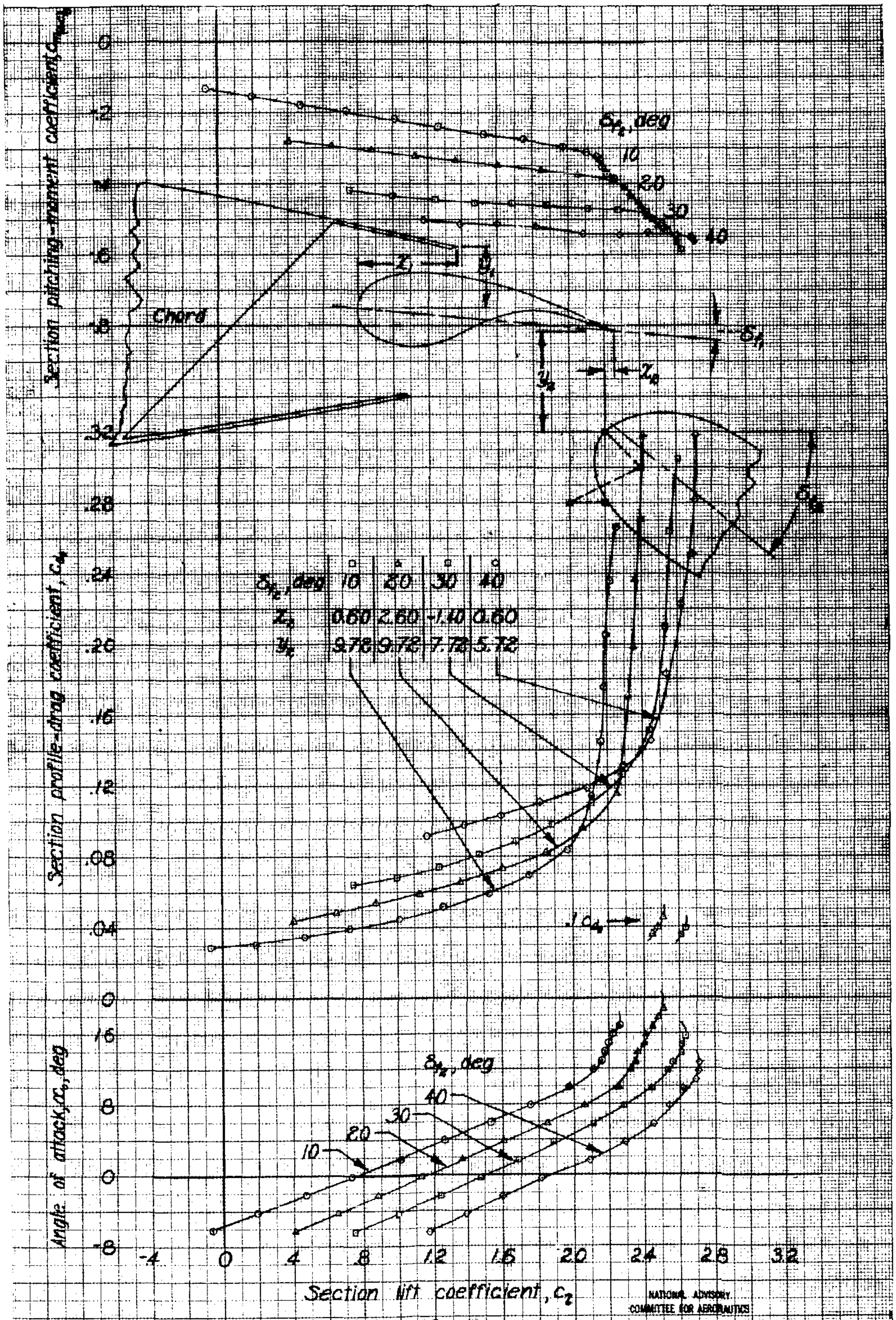

(a) Rear-flap positions for $c_{l_{max}}$.

Figure 12.- Aerodynamic section characteristics of NACA 23021 airfoil with a 0.32c double slotted flap. Position 1, $\delta_{f_1}=5°$. $x_1=5.70$; $y_1=3.45$. (Values of x_1, y_1 and x_2, y_2 are given in percent airfoil chord)

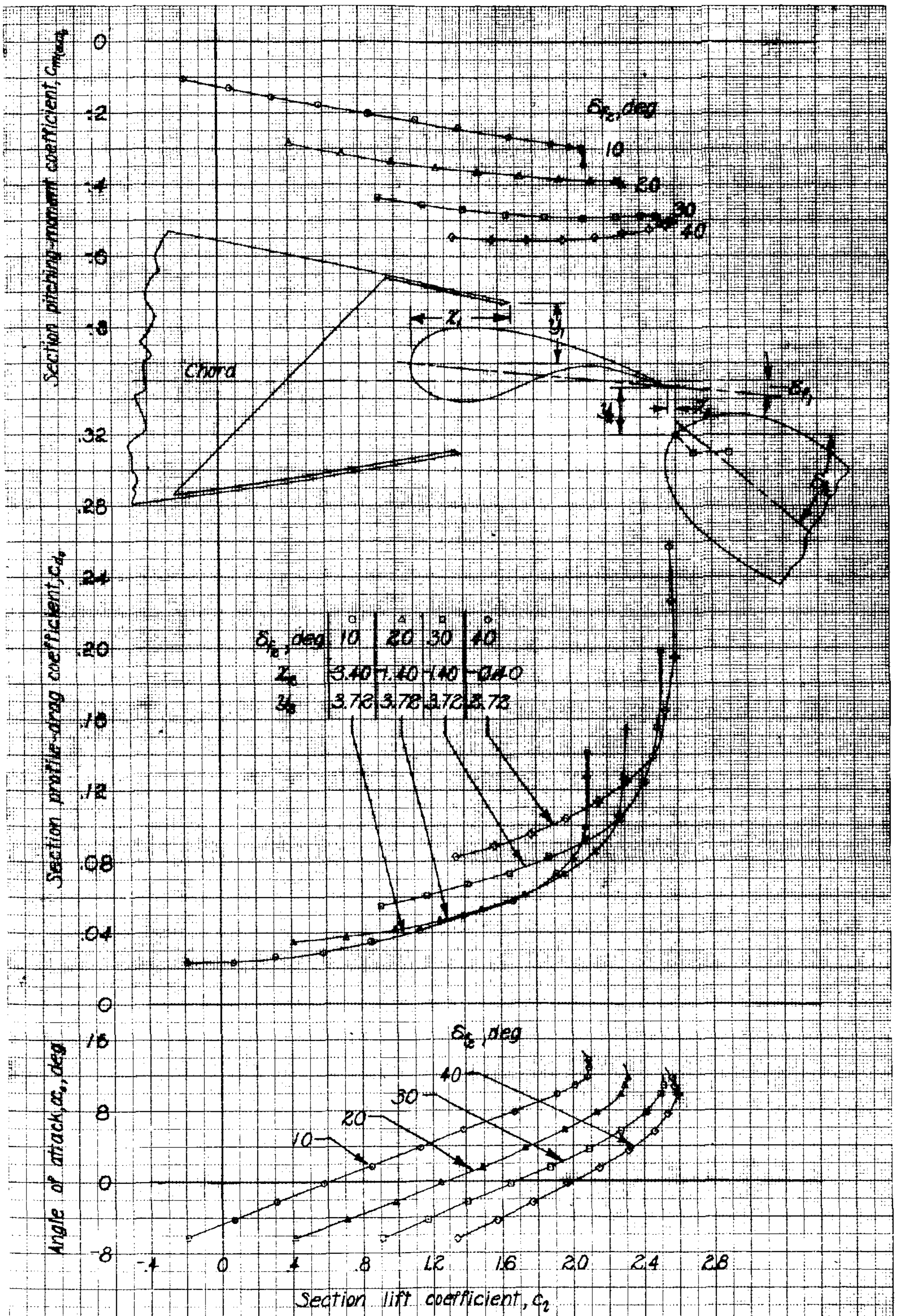

δ_{f_2}, deg	10	20	30	40
z_2	3.40	1.40	1.40	0.40
y_2	3.72	3.72	3.72	3.72

(b) Rear-flap positions for $c_{d_0\,min}$.

Figure 12.- Concluded.

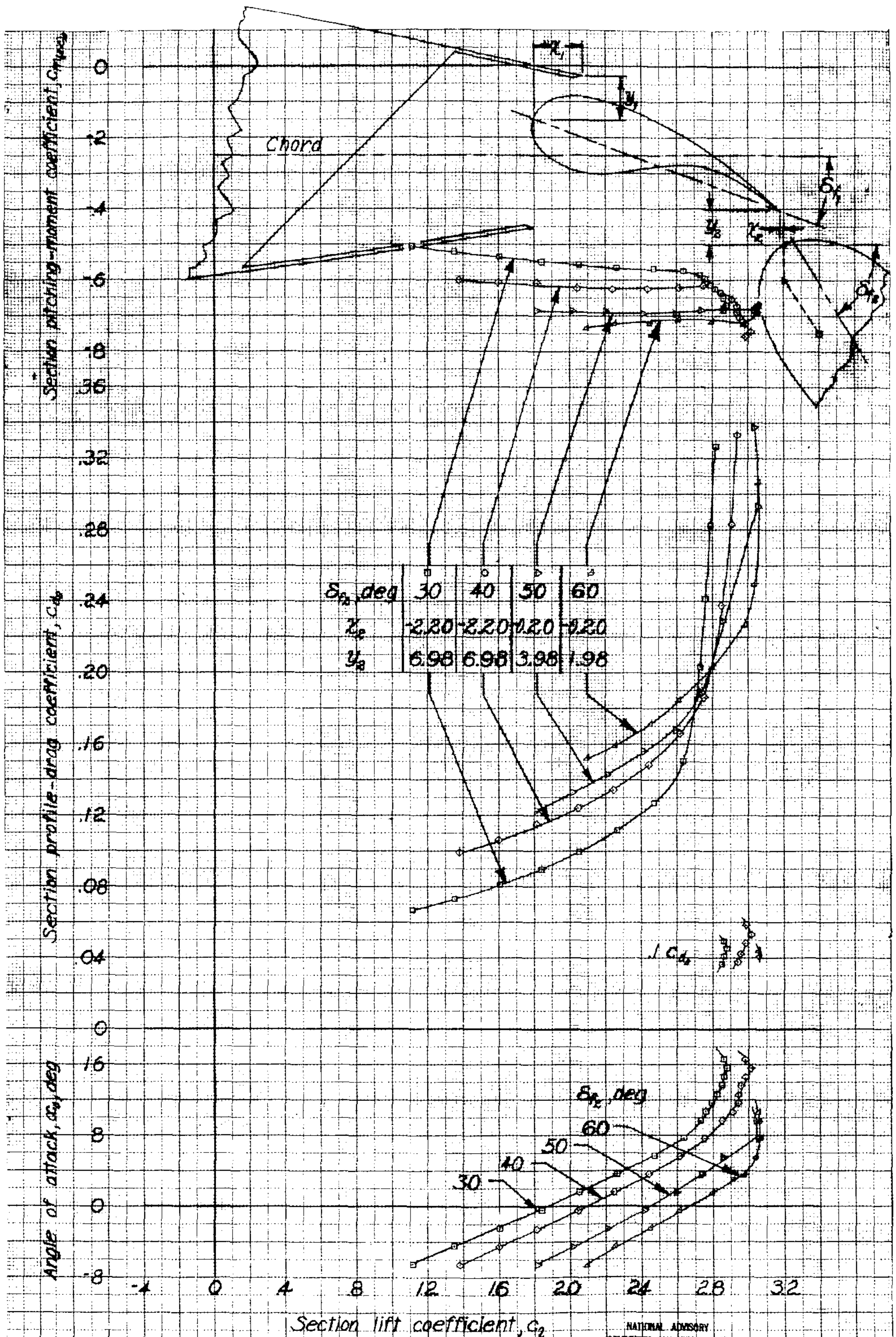

(a) Rear-flap positions for $c_{l_{max}}$

Figure 13.- Aerodynamic section characteristics of NACA 23021 airfoil with a 0.32c double slotted flap. Position 2; $\delta_{f_1}=20°$, $x_1=2.70$; $y_1=2.45$. (Values of x_1, y_1 and x_2, y_2 are given in percent airfoil chord.)

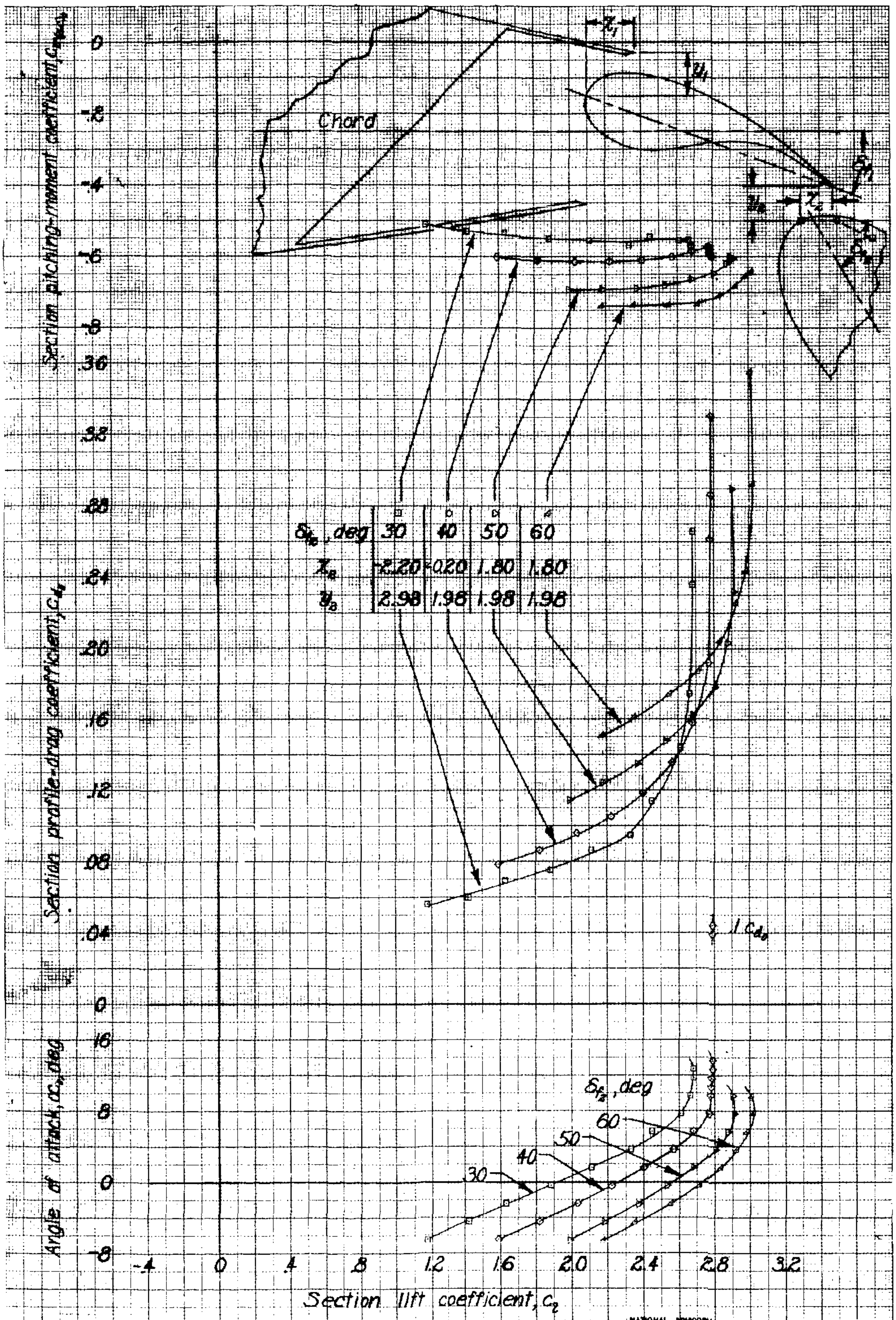

(b) Rear-flap positions for $c_{d_{0_{min}}}$.

Figure 13.- Concluded.

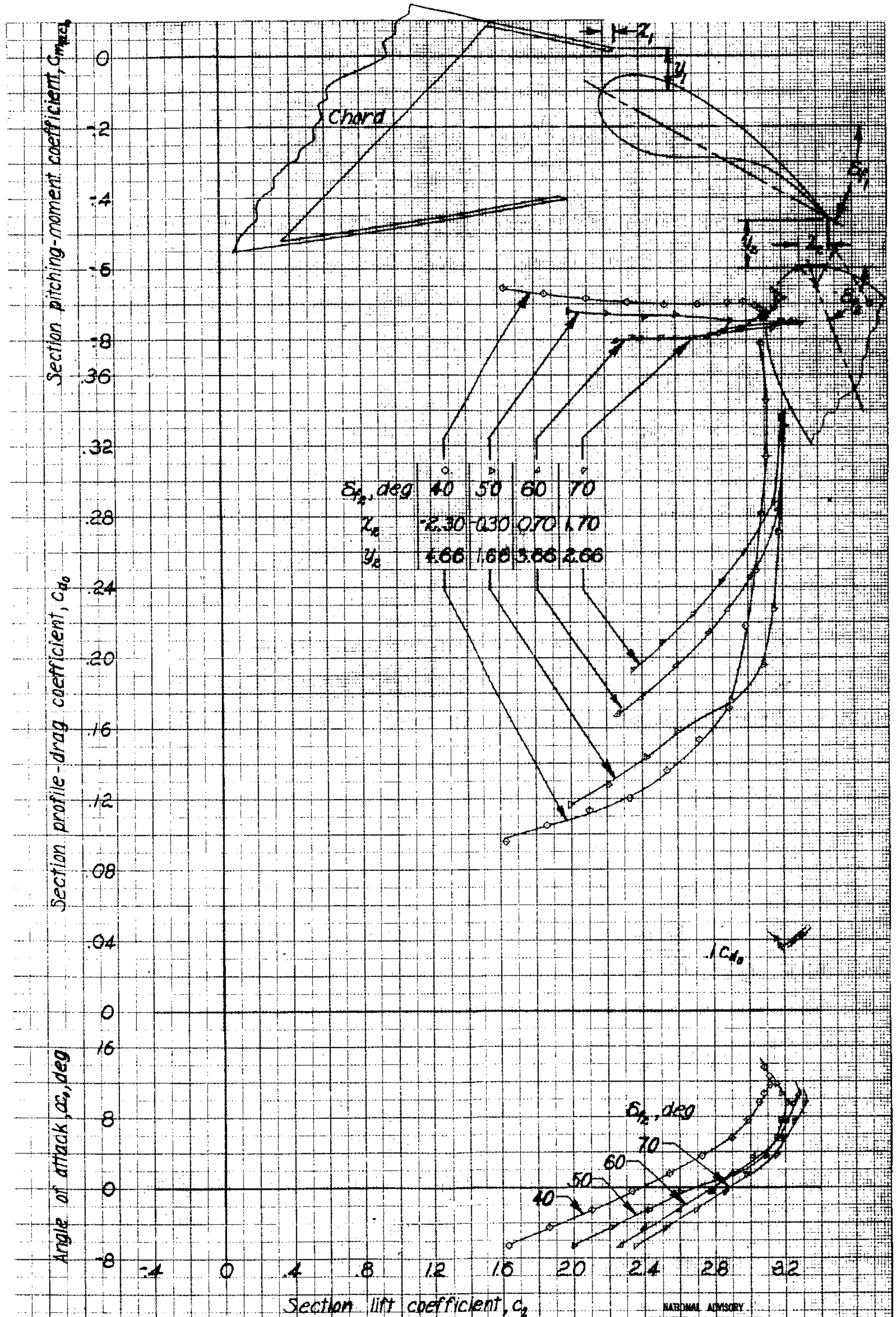

(a) Rear-flap positions for $c_{l_{max}}$.

Figure 14.- Aerodynamic section characteristics of NACA 23021 airfoil with a 0.32c double slotted flap. Position 3; $\delta_{f_1}=30°$, $x_1=0.70$; $y_1=2.45$. (Values of x_1, y_1 and x_2, y_2 are given in percent airfoil chord.)

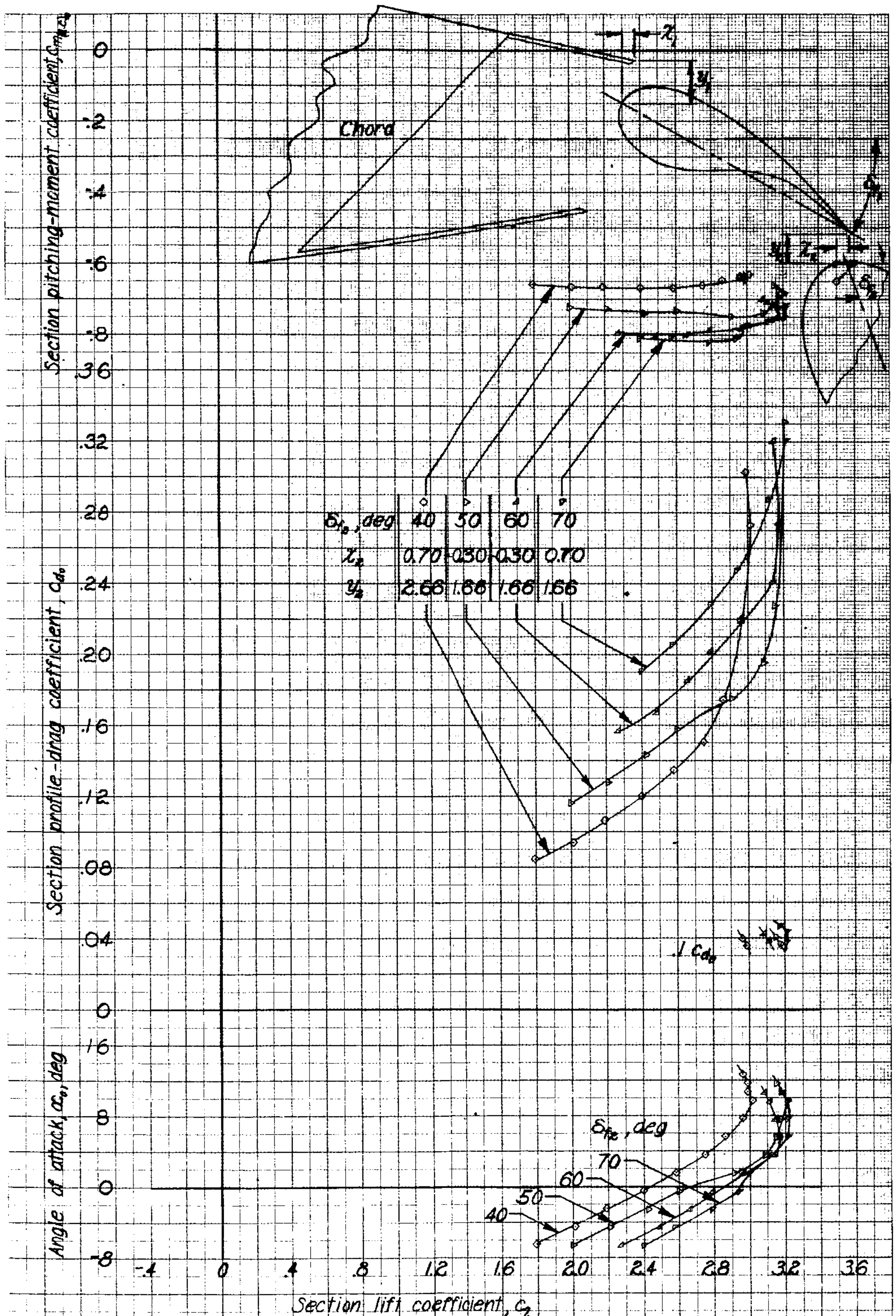

(b) Rear-flap positions for $c_{d_0 min}$.

Figure 14.- Concluded.

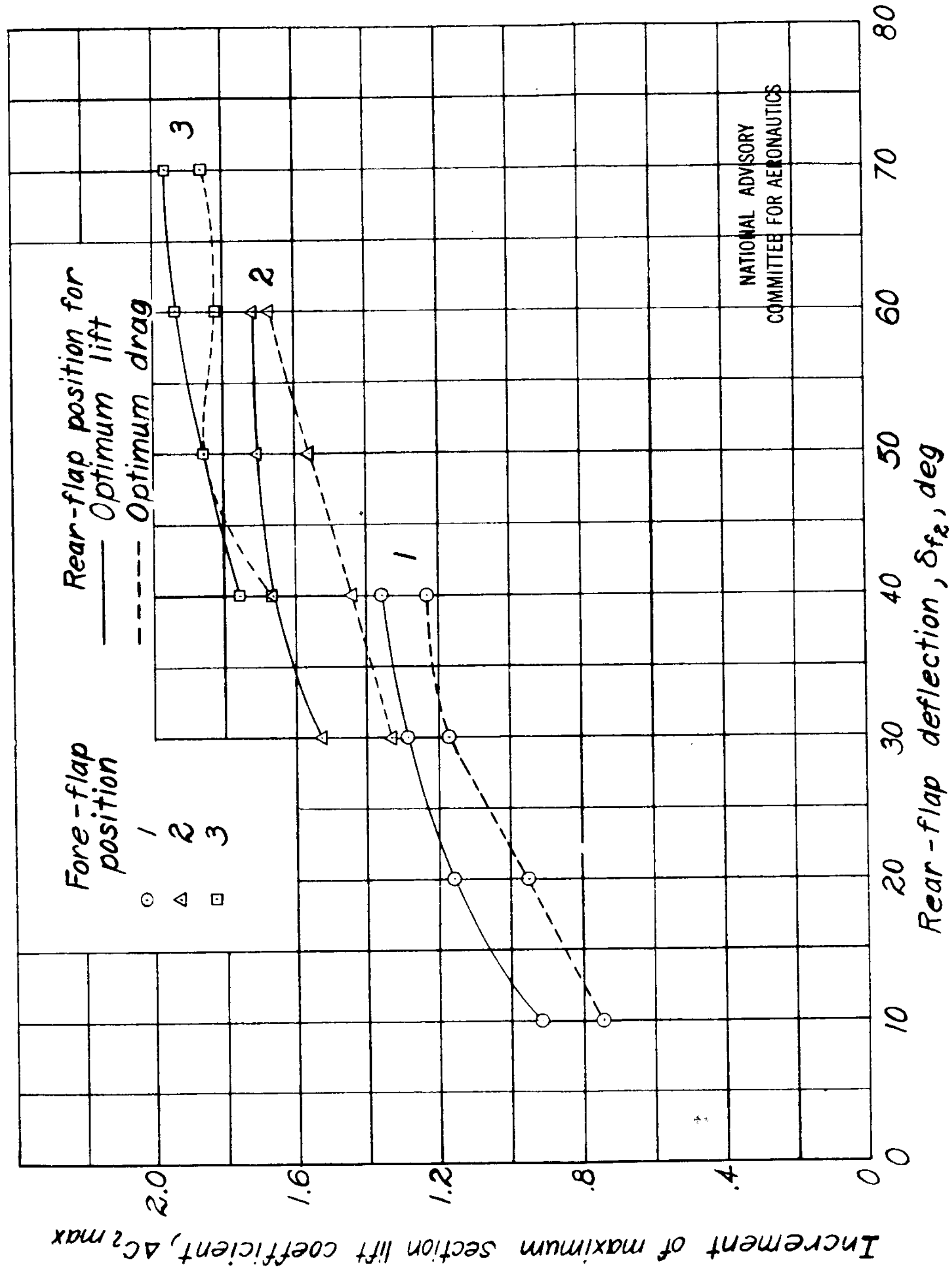

Figure 15.- Effect of rear-flap deflection on the increment of maximum section lift coefficient. The 0.32c double slotted flap on an NACA 23021 airfoil.

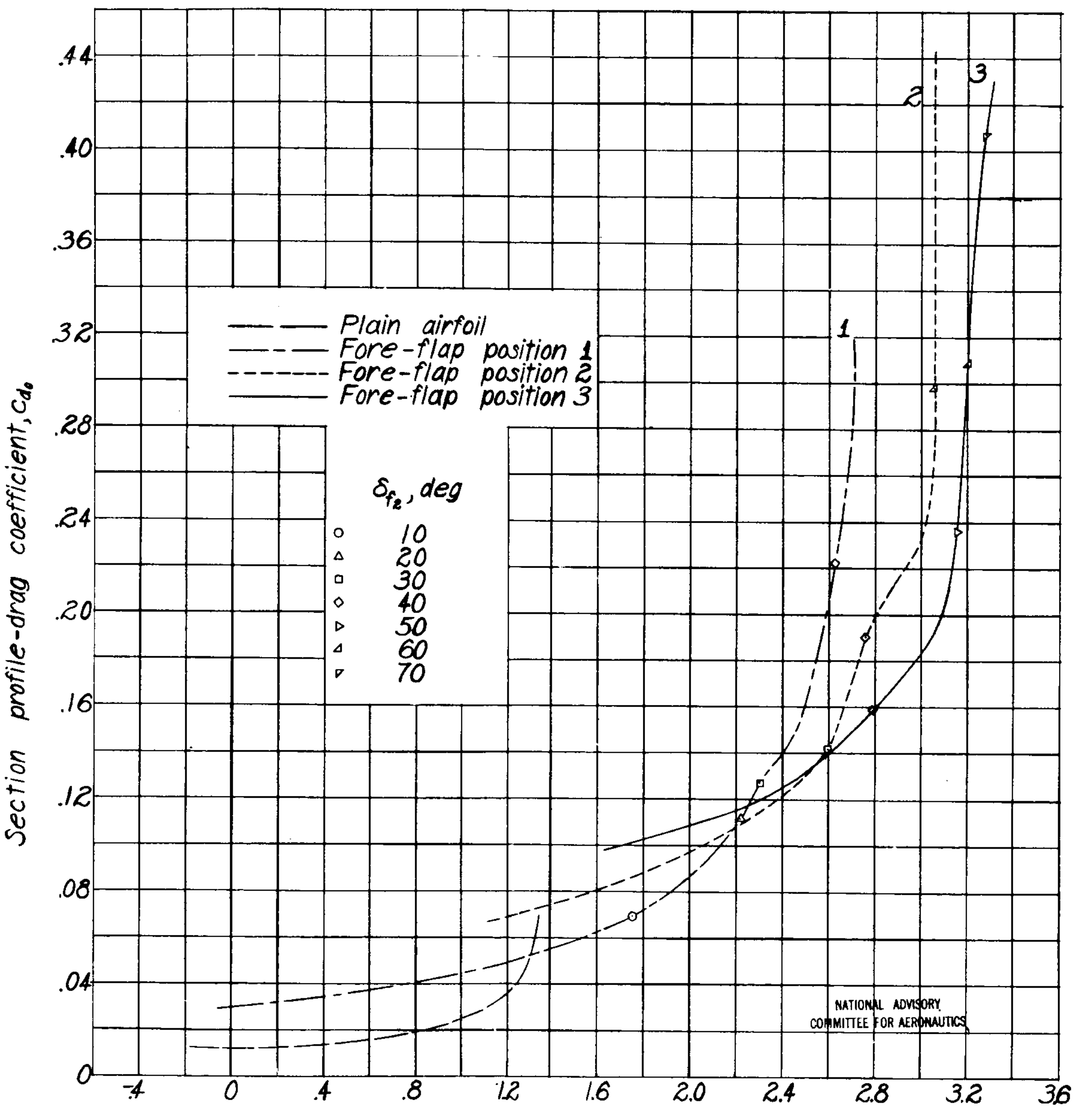

(a) Rear-flap positions for $c_{l_{max}}$.

Figure 16.- Profile-drag envelope polar curves for the NACA 23021 airfoil with a 0.32c double slotted flap.

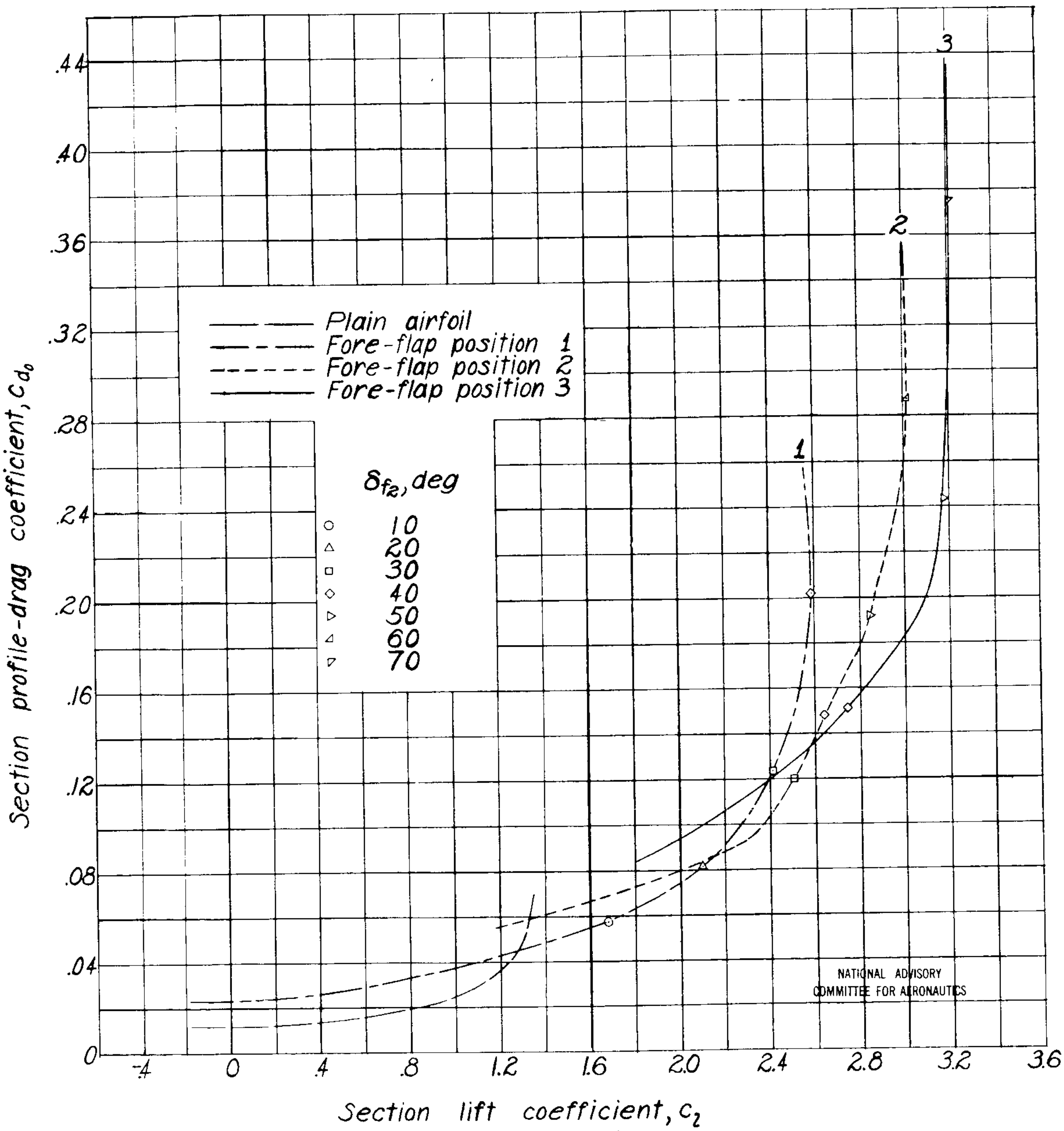

(b) Rear-flap positions for $c_{d_0 min}$.

Figure 16.- Concluded.

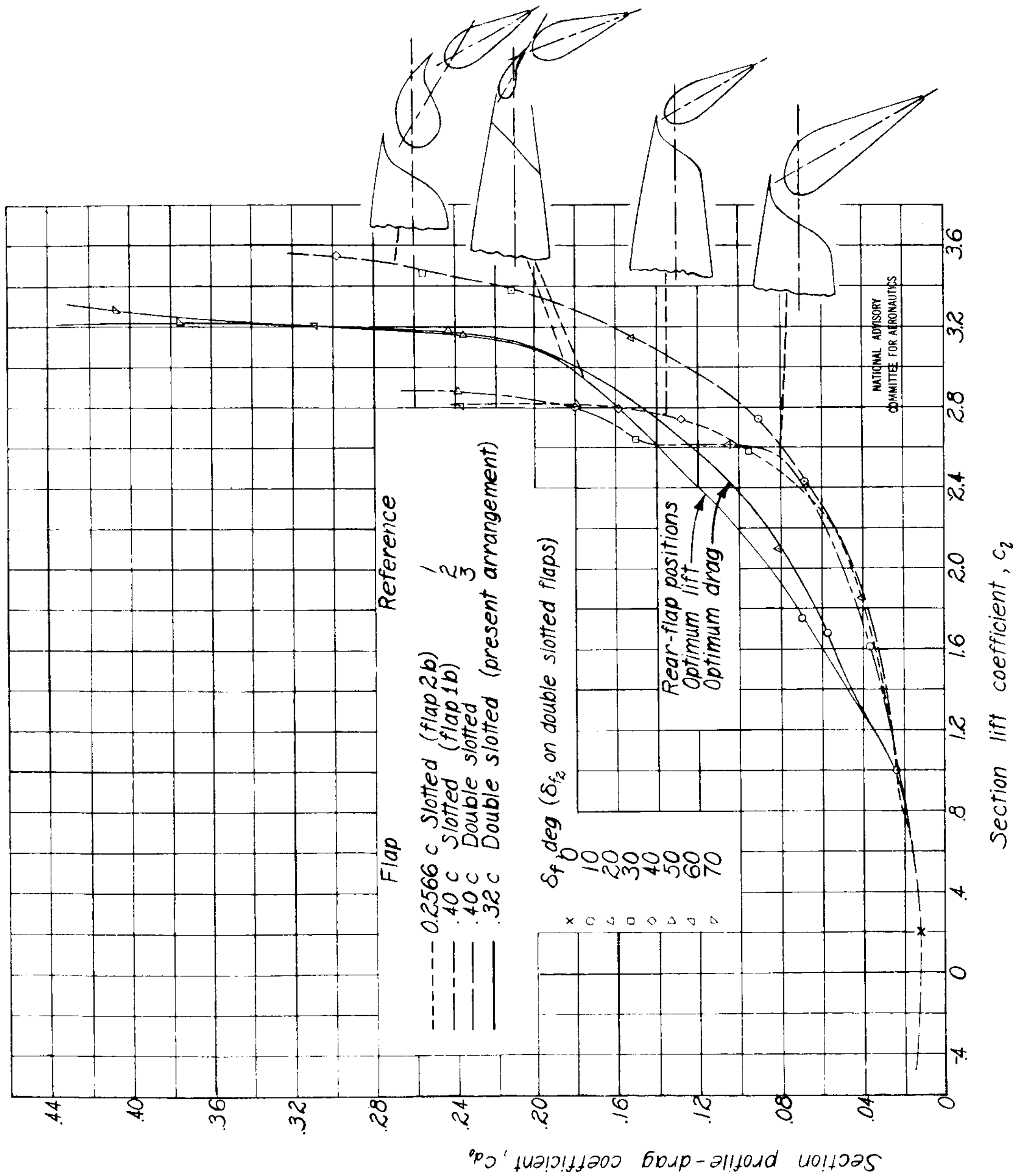

Figure 17.-Comparison of section profile-drag coefficients for several flap arrangements on the NACA 23021 airfoil.

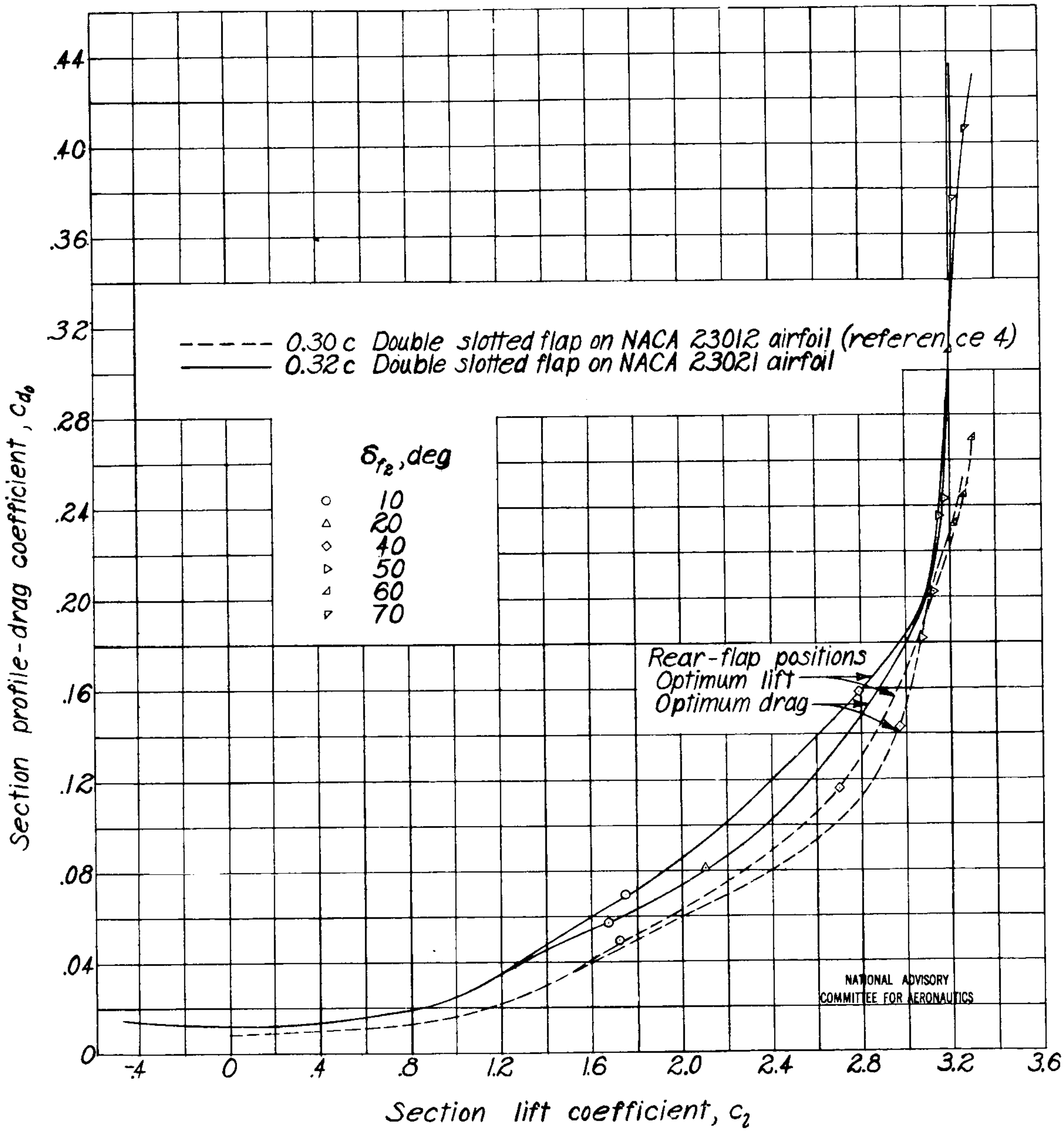

Figure 18.- Comparison of section profile-drag coefficients for similar double-slotted-flap arrangements on the NACA 23012 and NACA 23021 airfoils.

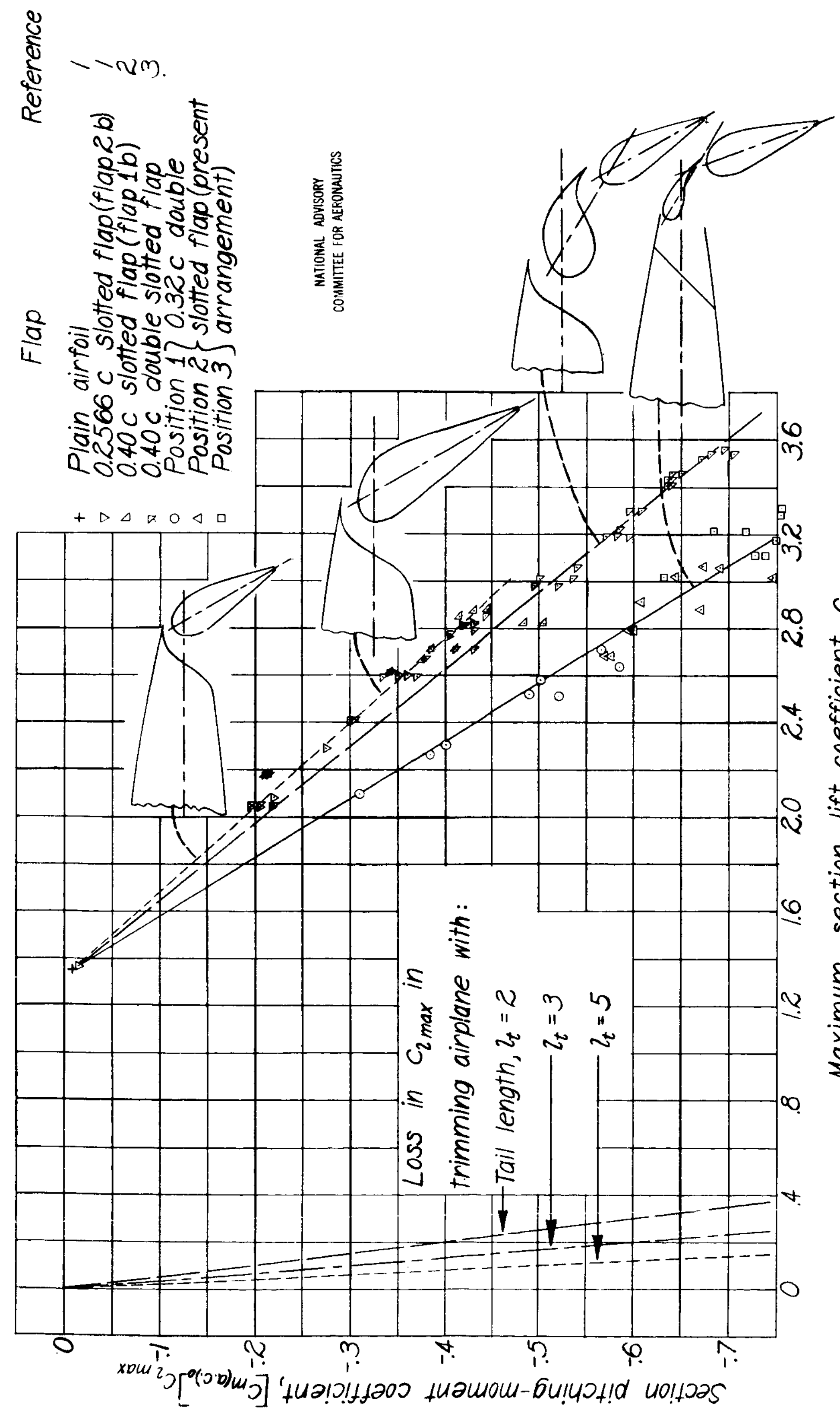

Figure 19.- Section pitching-moment coefficient at the maximum section lift coefficient for several flap arrangements on the NACA 23021 airfoil.

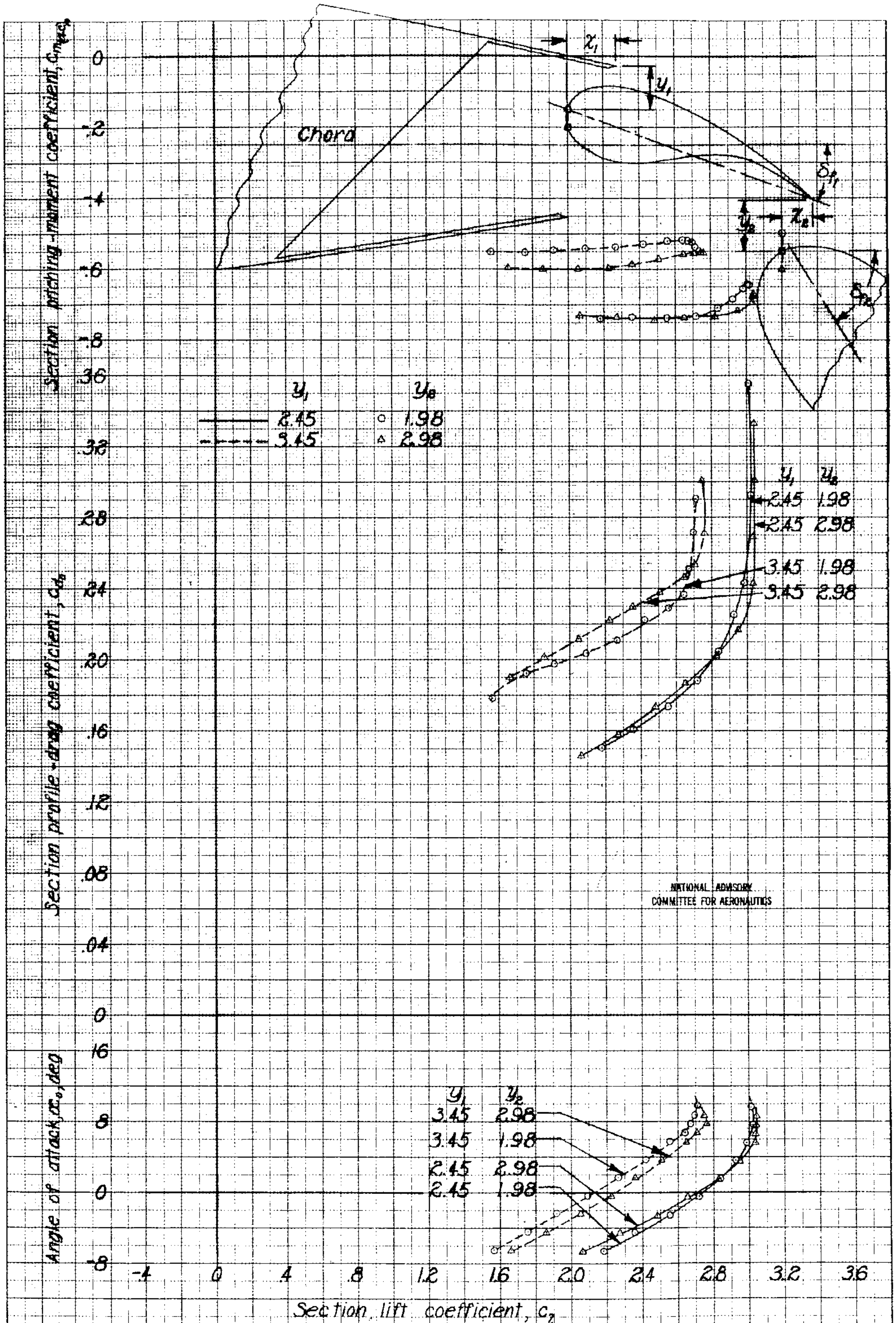

Figure 20.- Aerodynamic section characteristics of the NACA 23021 airfoil with a 0.32c double slotted flap showing the effect of moving the two flaps as a unit perpendicular to airfoil chord. $\delta_{f_1}=20°$, $\delta_{f_2}=60°$, $x_1=2.70$; $x_2=1.80$. (Values of x_1, y_1 and x_2, y_2 are given in percent airfoil chord.)

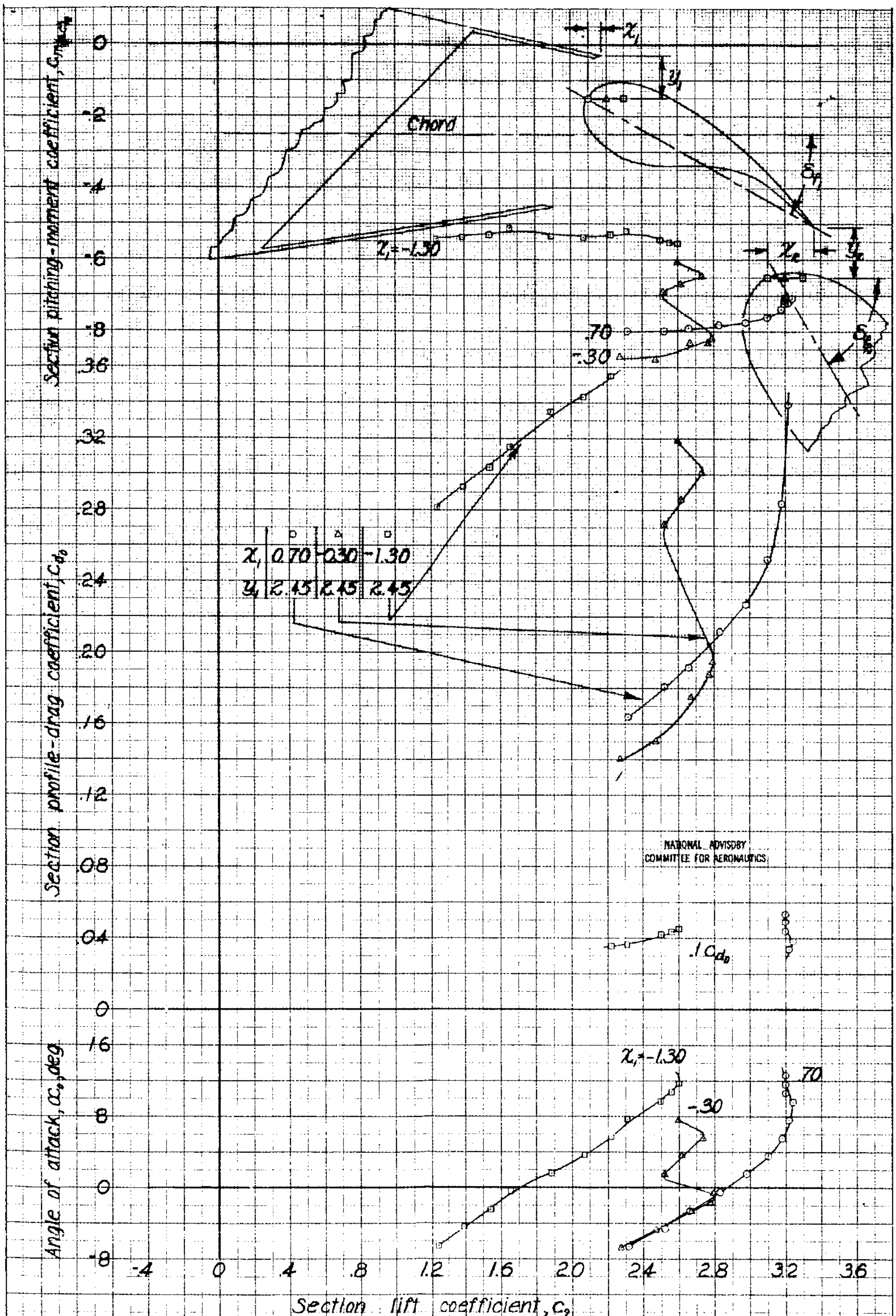

Figure 21.- Aerodynamic section characteristics of the NACA 23021 airfoil with a 0.32c double slotted flap showing the effect of moving the two flaps as a unit parallel to airfoil chord. $\delta_{f_1}=30°$; $\delta_{f_2}=60°$; $x_2=2.70$; $y_2=2.66$. (Values of x_1, y_1 and x_2, y_2 are given in percent airfoil chord.)

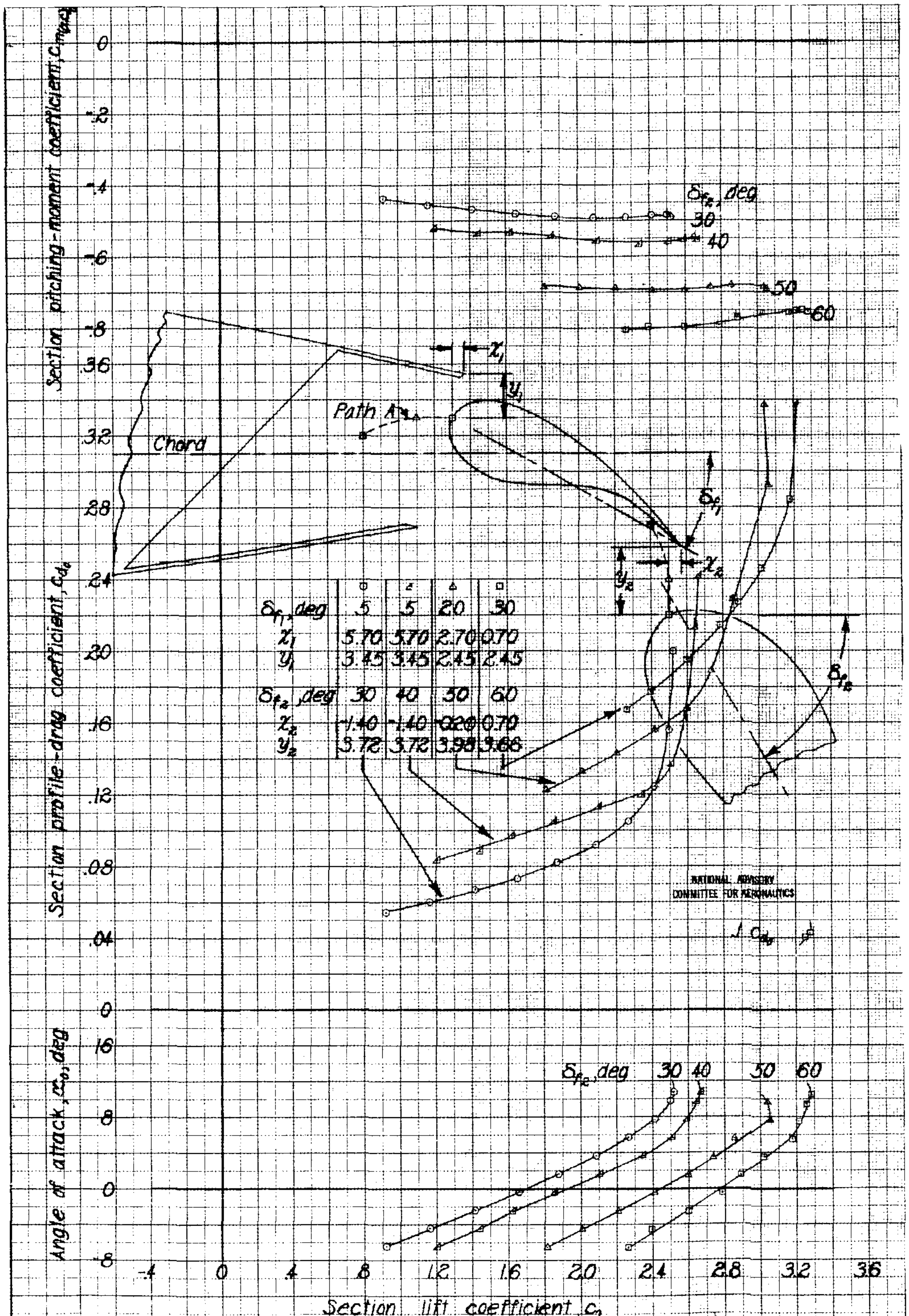

Figure 22.- Aerodynamic section characteristics of the NACA 23021 airfoil with a 0.32c double slotted flap showing the effect of moving the two flaps as a unit (approximately) from position 1 to position 3. Path A. (Values of x_1, y_1 and x_2, y_2 are given in percent airfoil chord.)

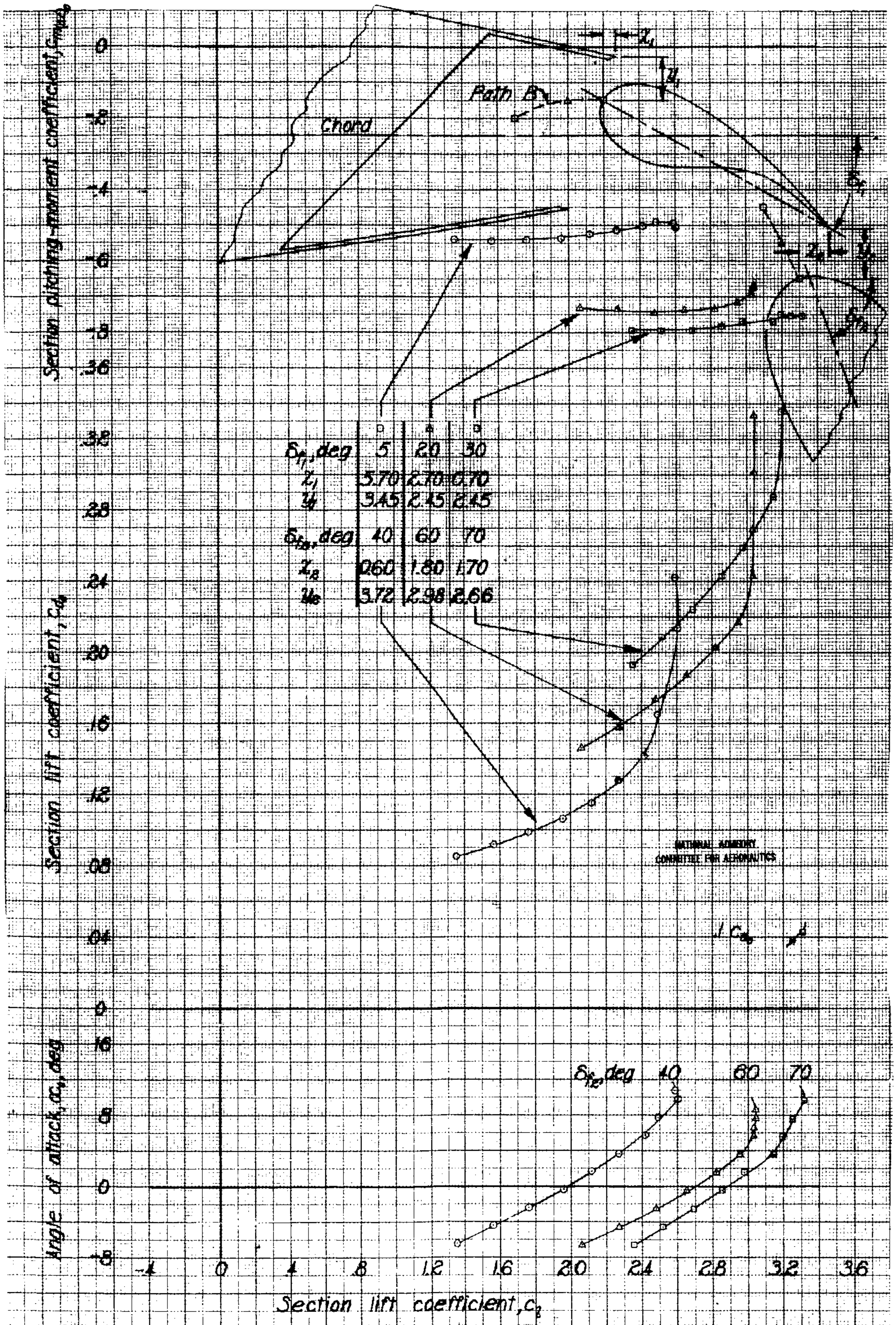

Figure 23.- Aerodynamic section characteristics of the NACA 23021 airfoil with a 0.32c double slotted flap showing the effect of moving the two flaps as a unit (approximately) from position 1 to position 3. Path B. (Values of x_1, y_1 and x_2, y_2 are given in percent airfoil chord.)

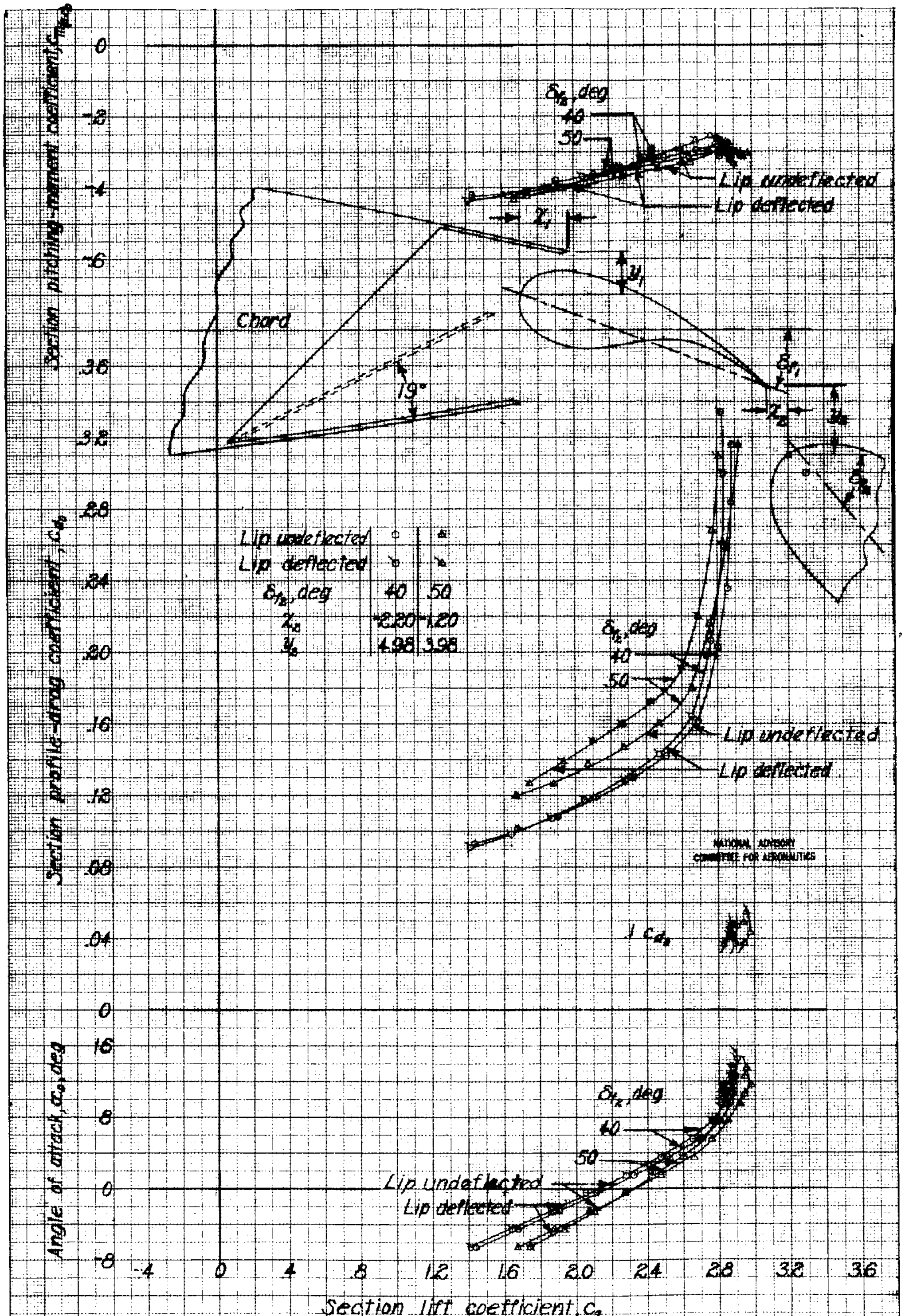

Figure 24.- Aerodynamic section characteristics of the NACA 23021 airfoil with a 0.32c double slotted flap showing the effect of deflecting the airfoil lower lip. Position 2; δ_{f_1}=20°; x_1=2.70; y_1=2.45. (Values of x_1, y_1 and x_2, y_2 are given in percent airfoil chord.)

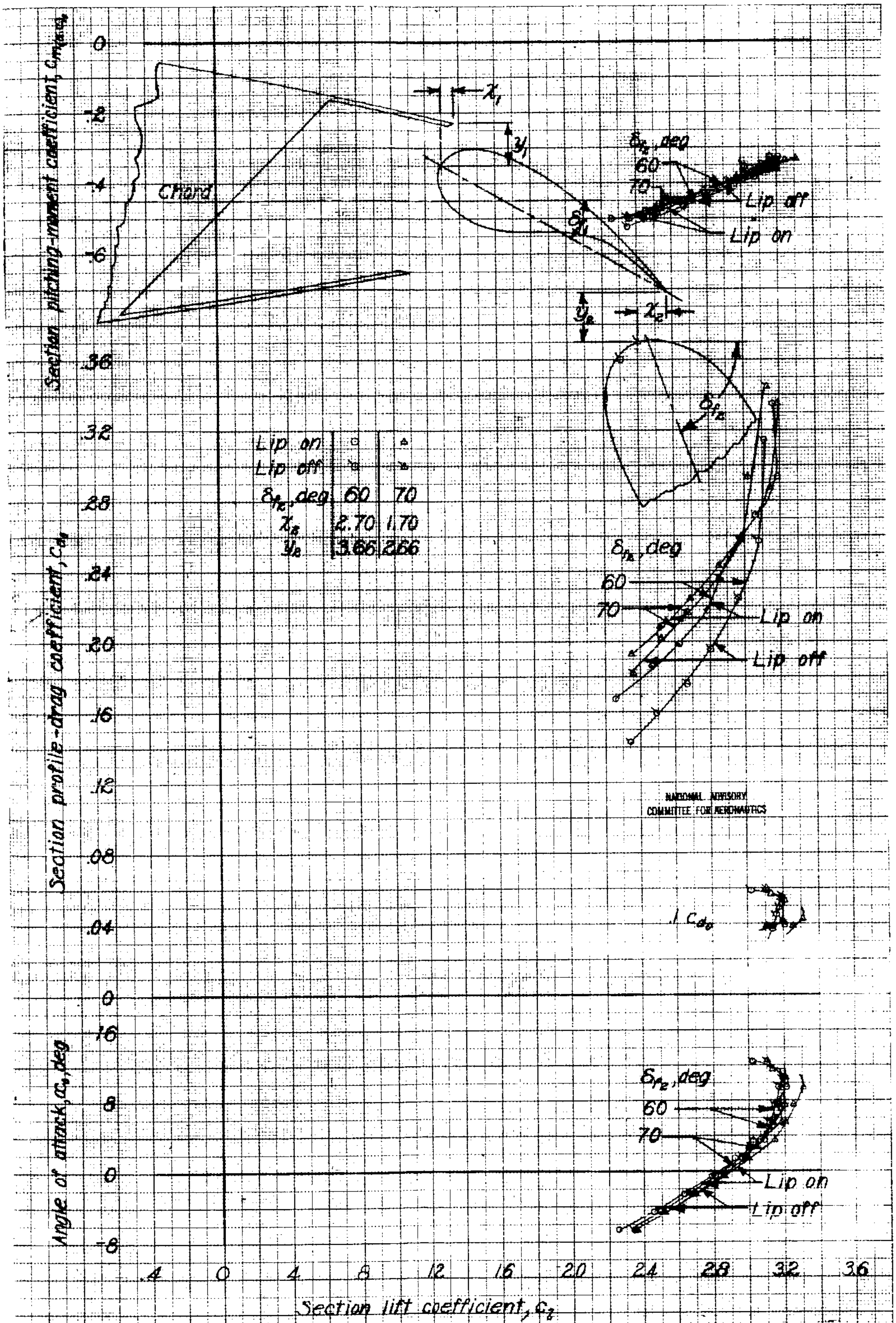

Figure 25.- Aerodynamic section characteristics of the NACA 23021 airfoil with a 0.32c double slotted flap showing the effect of removing the airfoil lower lip. Position 3; $\delta_f = 30°$, $x_1 = 0.70$, $y_1 = 2.45$. (Values of x_1, y_1, and x_2, y_2 are given in percent airfoil chord.)